Satellite Navigation Branch, ANG-E66

ADVANCED RECEIVER AUTONOMOUS INTEGRITY MONITORING PERFORMANCE ANALYSIS REPORT

August 2025

Report #13
Reporting Period: January 01, 2023 to March 31, 2023

FAA William J. Hughes Technical Center
Atlantic City International Airport, New Jersey 08405
http:/www.nstb.tc.faa.gov

DOCUMENT VERSION CONTROL

VERSION	DESCRIPTION OF CHANGE	DATE
0.1	Initial Draft	05/08/2025
0.2	Technical Edit	05/12/2025
0.3	Internal Peer Review	05/20/2025
1.0	Final Report	08/22/2025

EXECUTIVE SUMMARY

This is the first quarterly report of 2023 by the United States (U.S.) Federal Aviation Administration (FAA) documenting the performance of the Global Positioning System (GPS) and Galileo for use in Advanced Receiver Autonomous Integrity Monitoring (ARAIM). ARAIM will be used during aircraft flight operations to assure integrity of the satellite signals, which will permit aircraft to safely navigate worldwide in all phases of flight, including landing. The results in this report are intended for further discussion and validation of ARAIM standards. They are not intended for comparison to GPS performance commitments or Galileo performance commitments.

This report is produced by the FAA William J. Hughes Technical Center, Satellite Navigation Branch, ANG-E66, in Atlantic City, New Jersey.

For ARAIM, a global array of GNSS receivers is used to monitor signals from all GPS and Galileo (GPS/Galileo) satellites, and those signals are analyzed to determine performance. ARAIM standards are evolving, and performance requirements will be published in the future. In support of those requirements, signal monitoring is required to ensure that performance meets the standards, and to calculate the integrity parameters used to characterize the system. This report provides the current results of that monitoring.

This ARAIM Performance Analysis (PAN) Report #13 includes GPS and Galileo data and analysis for January 1, 2023 through March 31, 2023. For historical comparison and long-term trend analysis, performance data are presented from January 1, 2008 to March 31, 2023 for GPS, and January 1, 2020 to March 31, 2023 for Galileo. The report presents measured accuracy and integrity parameters and provides analysis to support the development of the GPS Integrity Support Message (ISM).

The following parameters are currently under consideration for ARAIM user calculation of service integrity: correlation time constant (t_{correl}), user range accuracy (URA)-independent overbound of nominal range bias errors ($b_{nom}0$), URA-dependent overbound of nominal range bias errors (γ_{nom}), specified probability of a single satellite fault (R_{sat}), probability of multiple common cause faults (P_{const}), mean fault duration (MFD), service level, and mask. In this report, the parameters R_{sat}, P_{const}, and MFD are considered the most mature; therefore, they are included. As standards mature, a complete definition of these parameters and their use will be available, and the report will provide the full complement of ARAIM parameters.

For GPS, the R_{sat} is currently 1×10^{-5}, the P_{const} is currently 1×10^{-8}, and the MFD is currently 1 hour. These values are consistent with GPS Constellation Service Provider (CSP) commitments. For Galileo, the R_{sat} is currently 3×10^{-5} and the P_{const} is currently 2×10^{-4}. These values are consistent with the Galileo Open Service Signal-In-Space Interface Control Document (OS SIS ICD) [1]. GPS satellites may be identified using either a space vehicle number (SVN) or a pseudorandom noise (PRN) number. SVN (sometimes written as SV) is an unambiguous number that is assigned when the spacecraft is built. PRNs are reused as vehicles are retired or added to the operational on-orbit constellation. This report uses the term SVN to uniquely identify the individual SV. These terms are the same as those used in Notice Advisory to Navstar Users (NANUs).

Galileo satellites may be identified using either a satellite name (GSAT) or a Satellite Vehicle Identification (SVID) number.

In this quarter, a fault was detected on SVN63 (PRN01) where the Signal-in-Space Range Error (SISE) exceeded 4.42 times the URA for approximately 180 minutes between 16:15 Coordinated Universal Time (UTC) and 19:15 UTC. The satellites health status remained healthy until 19:15 UTC. The maximum mean, 68%, and 95% values of the aggregated instantaneous SISE across 200 user locations in this quarter were -0.314 m on SVN64, 0.960 m on SVN72, and 2.240 m on SVN72, respectively.

Nominal clock and ephemeris errors for all GPS satellites were described conservatively by the broadcast URA with the exception of SVN63. In this quarter, URAs overbounded all nominal range errors with the maximum scale factor of 0.568 on SVN70. The URA value of 2.4 m was broadcast 92.752% of the time, in line with historical performance.

During this quarter, the monthly mean and 95% value of the aggregated instantaneous SISEs (for all GPS satellites across 200 user locations) were consistent with historical performance. All monthly means were under 0.480 m, and all the 95% values were under 2.450 m. The highest mean was 0.477 m on SVN73, and the highest 95% value was 2.420 m on SVN72.

The maximum mean, 68%, and 95% values of the aggregated instantaneous SISE for Galileo satellites across 200 user locations in this quarter were -0.958 m on GSAT0215, 1.000 m on GSAT0215, and 1.140 m on GSAT0215, respectively.

Nominal clock and ephemeris errors for all Galileo satellites were described conservatively by the Signal-In-Space Accuracy (SISA). In this quarter, URA overbounded all nominal range errors with the maximum scale factor of 0.499 on GSAT0210. The SISA value of 3.12 m was broadcast 99.829% of the time, in line with historical performance.

During this quarter, the monthly mean and 95% value of the aggregated instantaneous SISEs (for all Galileo satellites across 200 user locations) were consistent with historical performance. All monthly means were under 1.000 m, and all the 95% values were under 1.200 m. The highest mean was 0.959 m on GSAT0215, and the highest 95% value was 1.140 m on GSAT0215.

TABLE OF CONTENTS

LIST OF FIGURES

LIST OF TABLES

1. INTRODUCTION

This report documents the performance of GPS and Galileo, which support ARAIM for worldwide flight operations. ARAIM uses signals, validated for safety-of-flight use, from multiple satellite constellations without the use of an external augmentation system. ARAIM has the potential to reduce costs for service providers and aircraft operators. In its mature state, it will be able to provide worldwide precision approach capability to any location on earth and support expanded service to remote and unimproved areas.

This report is produced by the U.S. FAA William J. Hughes Technical Center, Satellite Navigation Branch (ANG-E66) in Atlantic City, New Jersey. The Satellite Navigation Branch also provides monitoring and reporting services on U.S. GPS performance and the FAA WAAS. These reports are titled "Global Positioning System Standard Positioning Service Performance Analysis Report" and "Wide Area Augmentation System Performance Analysis Report," respectively. Additionally, the branch monitors performance of the Galileo Global Navigation Satellite System (GNSS) and reports findings in the "Galileo Open Service Performance Analysis Report."

1.1 System Overview

ARAIM is intended to support navigation for en route, terminal, and approach flight operations by detecting hazardous faults in the underlying GNSS (i.e. GPS and Galileo) without the use of external augmentation systems. Making use of the increasing number of available ranging satellites, ARAIM determines the probabilities of one or more simultaneous fault occurrences and calculates an integrity level. ARAIM updates are contained in the ISM, provided by ground monitoring networks that maintain continuous worldwide GNSS coverage. A more detailed operational description is found in the ARAIM Concept of Operation [2].

1.2 Purpose

The purpose of this report is to document the ARAIM-related performance parameters of the core constellations that will support ARAIM flight operations and to provide that information to users, operators, and regulators.

1.3 Scope

This report currently focuses on the ARAIM-related performance parameters of GPS and Galileo and the ability to support worldwide flight operations using ARAIM. For future operations, ARAIM is planned to be implemented in phases, first for horizontal navigation, and later expanded to include vertical navigation. As those changes are implemented, these quarterly reports will also be expanded to reflect the evolving nature of ARAIM applications.

1.4 Report Layout

This report presents several types of ARAIM performance information, including nominal GNSS accuracy and statistical distributions, satellite faults and estimated fault rates, historical performance, and verification of some of the underlying assumptions of the defining algorithms.

A description of the ARAIM ISM parameters and constellation requirements are presented in Section 2.

Data is presented in Section 3, including the data source, data cleansing, processing, and analysis. This section also discusses the partitioning of the data and some of the data limitations.

Nominal GNSS performance is presented in Sections 4 and 5, including nominal errors and URA, along with statistical error distributions and URA bounding analysis. These sections also provide correlation analysis of the nominal error at each user position.

Satellite faults are presented in Section 6, including estimated fault rates and historical fault information.

Section 7 contains a list with descriptions of any significant or unusual events, such as satellite or monitoring system failures or other unexpected events that impact performance.

The list of glossary terms and acronyms is presented in APPENDIX A: GLOSSARY AND ACRONYMS.

A summary of the January 25, 2023 SVN63 (PRN01) fault event is presented in APPENDIX B: SVN63 (PRN01) Fault.

2.   ISM PARAMETER OFFLINE MONITORING

The ARAIM ISM parameter offline monitoring effort provides for the monitoring of the safety parameters that will be communicated to users through the ISM, including the following:

- An overbound of the probability or rate of single satellite faults (P_{sat} or R_{sat})
- An overbound of the probability or rate of multiple simultaneous faults (P_{const} or R_{const})
- An overbound of nominal range errors (URA)
- A URA-independent overbound of nominal range bias errors ($b_{nom}0$)
- A URA-dependent overbound of nominal range bias errors (γ_{nom})
- An overbound of the MFD
- t_{CORREL}
- Service Level
- Mask

ISM parameter values are unique to each satellite constellation. These parameters are based on CSP commitments and performance history. They must conservatively describe the true satellite behavior to be used to predict integrity. Constellation performance is monitored continually to ensure consistency with those commitments.

If required, the results of offline monitoring of the γ_{nom}, t_{CORREL}, $b_{nom}0$, service level, and satellite mask will be included in future reports as standards evolve.

Table 2-1 is a copy of the integrity guarantee as defined in the GPS Standard Positioning Service (SPS) Performance Standard (PS) [3]. The SPS PS states that the probability of a satellite fault

will be no greater than 1x10^{-5} per hour. The commitment further states that users will be notified of major service failures, or the space vehicle (SV) will be removed from service within an average of 1 hour.

Table 2-1. GPS SPS Instantaneous User Range Error Integrity Standards [3]

Signal-in-Space (SIS) Integrity Standard	Conditions and Constraints
• Each SPS SIS Component Combination per Table 2.2-2 in the GPS SPS Performance Standard [3]: • ≤1×10^{-5} Probability Over Any Hour of the SPS SIS Instantaneous User Range Error (URE) Exceeding the Not-To-Exceed (NTE) Tolerance Without a Timely Alert	• Applies to any trackable and healthy SPS SIS • SPS SIS URE NTE tolerance defined to be 4.42 times the relevant Integrity Assured User Range Accuracy (IAURA) value currently broadcast by the satellite • Given that the maximum SPS SIS instantaneous URE did not exceed the NTE tolerance at the start of the hour • Unalerted Misleading Signal Information (UMSI) occurs if no timely alert issued after SPS SIS URE NTE tolerance exceeded • Worst case for delayed alert is 6 hours • Neglecting single-frequency (SF) ionospheric delay model errors
Instantaneous P_{sat} and P_{const}	**Conditions and Constraints**
• ≤1×10^{-5} Fraction of Time When the SPS SIS Instantaneous URE Exceeds the NTE Tolerance Without a Timely Alert (P_{sat}) • ≤1×10^{-8} Fraction of Time When the SPS SIS Instantaneous URE from Two or More Satellites Exceeds the NTE Tolerance Due to a Common Cause Without a Timely Alert (P_{const})	• Applies across all trackable and healthy SPS SIS • SPS SIS URE NTE tolerance defined to be ±4.42 times the relevant IAURA value currently broadcast by the satellite • Average case for delayed alert is 1 hour • Neglecting SF ionospheric delay model errors

Table 2-2 is compiled from the integrity guarantee as defined in the Galileo Open Service Service Definition Document (OS SDD) [4]. The OS SDD states that the probability of a satellite fault will be no greater than 3×10^{-5} per hour.

Table 2-2. Galileo OS SDD Instantaneous User Range Error Integrity Standards [4]

Galileo Probability of Single SIS Fault	Conditions and Constraints
• $P_{sat} \leq 3 \times 10^{-5}$	• SISE $>k \times$ Galileo URA (factor k is 4.17 for P_{sat} $3 \times 10^{-5)}$) • At any location in the respective visibility areas of the affected satellites • Applicable to both OS single frequency users (E1 and E5a) and dual frequency users (E1-E5a combination), starting from healthy supporting signals • Propagation and user contributions excluded
Galileo Probability of Constellation SIS Fault	**Conditions and Constraints**
• $P_{const} \leq 2 \times 10^{-4}$	• SISE $>k \times$ Galileo URA (factor k being 4.17) for two or more satellites due to a common failure. • At any location in the respective visibility areas of the affected satellites • Applicable to both OS single frequency users (E1 and E5a) and dual frequency users (E1/E5a combination), starting from healthy supporting signals • Propagation and user contributions excluded

3.   DATA

3.1   Data Source and Rate

The offline analysis in this report uses two sources of input data: broadcast navigation data and post-processed precise data. The broadcast navigation data consists of satellite orbit and clock parameters and includes URA values that indicate the expected level of accuracy. The precise data is used as the truth reference and consists of ephemerides and clock parameters.

A subset of the GPS broadcast LNAV data and a subset of the Galileo navigation message FNAV is available from the International GNSS Service (IGS) in Receiver Independent Exchange (RINEX) navigation file format [5].

Precise GPS ephemerides and clock are available from the National Geospatial-Intelligence Agency (NGA) in the Standard Product #3 (SP3) format and has an accuracy of approximately 10 centimeters (cm) [6]. Precise Galileo ephemerides and clock are available from Center for Orbit Determination in Europe (CODE).

This report includes historical GPS constellation performance from January 1, 2008 to March 31, 2023. Data was analyzed for every 15-minute interval from January 1, 2008 to February 26, 2012 and every 5-minute interval from February 26, 2012 until March 31, 2023. The data intervals are determined by capabilities of the IGS and NGA data sources.

This report also includes historical Galileo constellation performance from January 1, 2020 to March 31, 2023. Data comparisons between the broadcast ephemeris and the precise position were analyzed in 5-minute intervals. The data intervals are determined by capabilities of IGS and CODE data sources.

3.2   Data Collection and Cleansing

A customized tool is used to automate the data downloads on a daily basis. All data are protected by checksums or other basic integrity checks. GPS broadcast navigation data is downloaded from the two IGS archive sites: the Crustal Dynamics Data Information System (CDDIS) [7] and the Scripps Orbit and Permanent Array Center (SOPAC) [8]. Precise data is downloaded from the NGA server [9]. Galileo broadcast navigation data and precise orbit data are downloaded from CDDIS.

The broadcast navigation data, as received in RINEX format from IGS, sometimes contains defects (such as duplications, inconsistencies, discrepancies, and errors) that can cause false anomalies. A cleansing algorithm is applied to the IGS data to generate "validated" navigation messages, which have as many of these defects removed as possible. This process is based on the algorithm described by Heng [10].

3.3   Error Computation and Anomaly Detection

For each time step where precise data is available, the most recent prior validated broadcast navigation data are used to propagate the satellite orbits and clocks. To account for clock offset in the precise product, at each epoch, the clock residuals between healthy precise and broadcast products are filtered for outliers; then, a mean correction is applied to the NGA/CODE precise clock estimates. At each data point for which both sources indicate a healthy signal and valid data within the fit interval, the satellite position error is determined by calculating the difference between the NGA/CODE-derived reference value and the calculated, propagated satellite position, in Earth-Centered, Earth-Fixed (ECEF) coordinates. The errors are segregated into radial, along-track, and cross-track (RAC) errors. The satellite position error is also projected onto Earth at each epoch to produce the maximum projected error (MPE) and projected along the lines of sight to individual user locations on Earth to produce user projected error (UPE). MPE and UPE are two forms of SISE that are used to evaluate the error distributions.

In this report, 200 evenly distributed user locations around the globe were used to calculate UPE. This density was determined to be sufficient such that a value within 2 cm of the actual MPE will be observed at one or more of the user locations [11]. MPE is computed for each satellite, at each epoch. UPE is computed for each of the 200 user locations, for each satellite in view, for each epoch. A mask angle of 5 degrees is used for MPE and UPE computations. UPEs across satellites are also combined to create a position error at each of the 200 user locations, at each epoch, and a sum of squared residuals statistic is computed. Figure 3-1 shows the 200 MPE user locations.
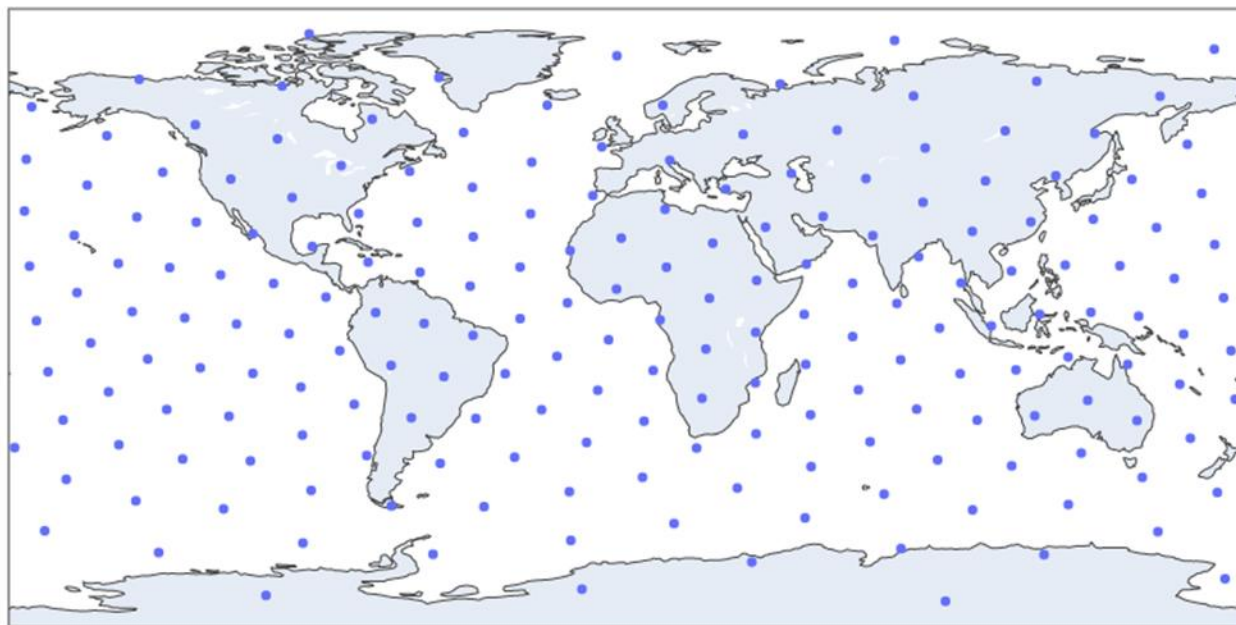
Figure 3-1. MPE User Locations

The GPS SPS PS [3] considers an integrity error has occurred if the SISE is greater than 4.42* URA, where URA is the broadcast accuracy estimate (see Table 2-1). The Galileo OS SDD [4] considers an integrity error has occurred if the SISE is greater than 4.17*URA, where URA is less than or equal to 7.5 meters for single frequency (see Table 2-2). This report uses a conservative criterion, MPE, to determine if an error has occurred. A potential GPS SIS anomaly is reported when MPE exceeds the 4.42* URA threshold, and a potential Galileo SIS anomaly is reported when MPE exceeds the approximately 31-meter threshold.

Figure 3-2 shows an overview of GPS data availability for the individual months in this quarter. The vertical axis identifies each satellite by their SVN and block type. Each horizontal line indicates health and status for an individual satellite. Green indicates that the vehicle was set healthy, broadcast ephemeris was received, and a valid comparison to the precise ephemeris was obtained. Blue indicates that the vehicle was set unhealthy; therefore, no comparison was available. Purple indicates that no broadcast ephemeris was obtained from the IGS database, and orange indicates that the precise ephemeris was not obtained. In each of those cases, the state of the vehicle was undetermined. The final case, shown by a red circle, indicates that a fault anomaly was detected, and the event will be described in Table 7-1.
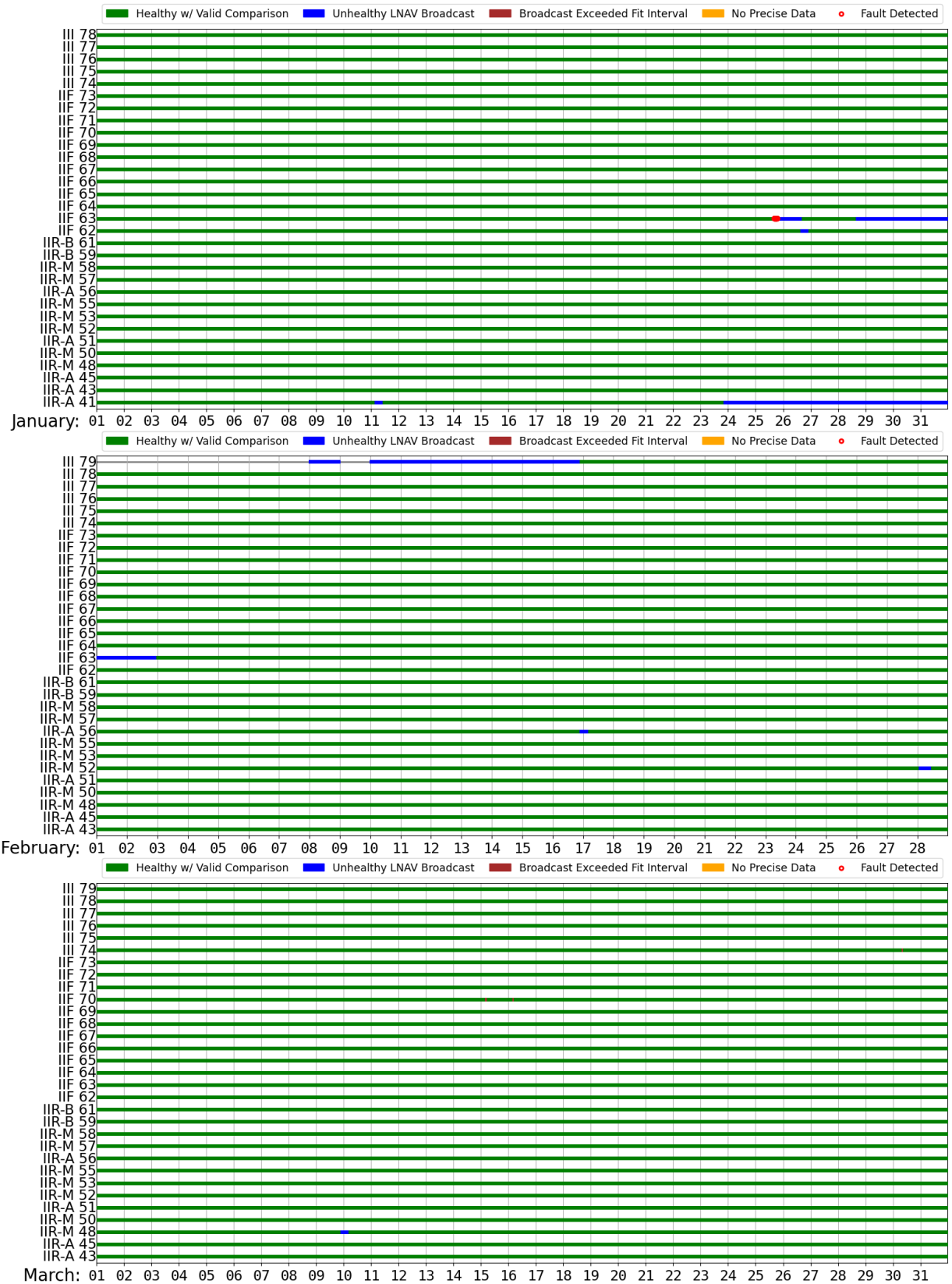
Figure 3-2. GPS Satellite Data: 1st Quarter 2023

Table 3-1 shows the sample counts and the percentages of GPS satellite data for this quarter. A total of 794,402 samples were evaluated this quarter and 1 fault was detected on SVN63 (PRN01) with a duration of approximately 180 minutes. The data that was not evaluated corresponded to satellites flagged "Unhealthy," data that exceeded the 4-hour fit interval, or data that was flagged in the precise position product. The 35 data samples where the normalized MPE exceeded 4.42 on SVN63 (PRN01) between 16:15 UTC and 19:15 UTC were not evaluated. During the quarter, several satellites were set to "Unusable" for short periods of time. A complete list of NANUs is available in Table 7-1.

Table 3-1. GPS Satellite Data: 1st Quarter 2023

Data Evaluation	Number of Samples	Percentage of Total
Valid Data Evaluation	794402	97.090%
No Evaluation due to SV Unhealthy	23752	2.903%
No Evaluation due to Exceeding 4-hour Fit Interval	9	0.001%
No Evaluation due to Precise Data Event Flag	10	0.001%
No Evaluation due to Broadcast Data Unavailable	0	0.000%
No Evaluation due to Precise Data Unavailable	0	0.000%
Faults	35	0.004%

Figure 3-3 shows an overview of Galileo data availability for the individual months in this quarter. The vertical axis identifies each satellite by their Satellite Name (GSAT) and Full Operational Capability (FOC) block. Each horizontal line indicates health and status for an individual satellite. Green indicates that the vehicle was set healthy, the vehicle was not marginal, broadcast ephemeris was received, and a valid comparison to the precise ephemeris was obtained. Blue indicates that the vehicle was set unhealthy or marginal; therefore, no comparison was available. Purple indicates that no broadcast ephemeris was obtained from the IGS database, and orange indicates that the precise ephemeris was not obtained. In each of those cases, the state of the vehicle was undetermined. The final case, shown by a red circle, indicates that a fault anomaly was detected, and the event will be described in Table 7-2.
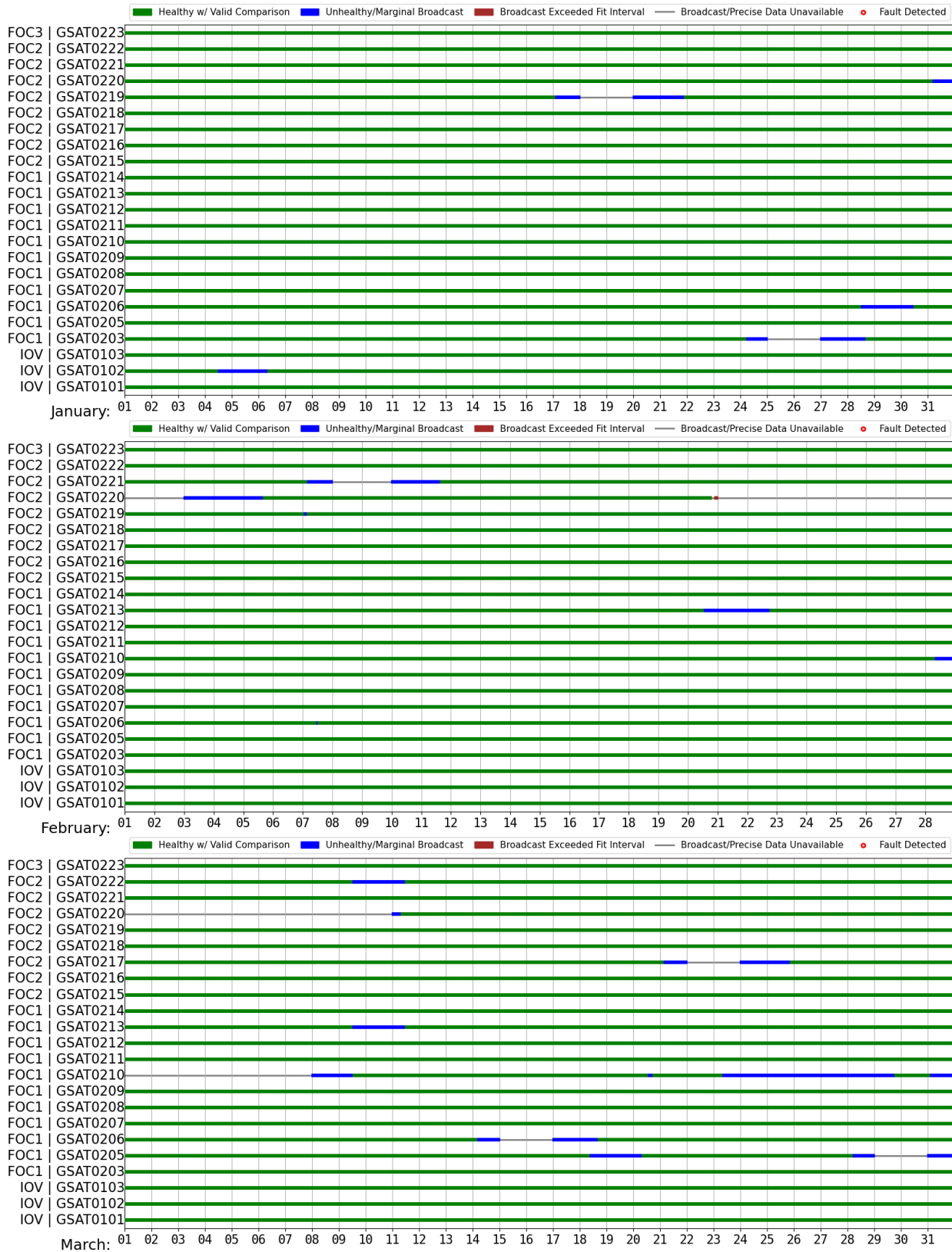
Figure 3-3. Galileo Satellite Data: 1st Quarter 2023

Table 3-2 shows the sample counts and the percentages of Galileo satellite data for this quarter. A total of 573,501 samples were evaluated this quarter. The data that were not evaluated corresponded to satellites flagged "Unhealthy," satellites determined to be "Marginal," data that exceeded the 4-hour fit interval, or data that was flagged in the precise position product. During the quarter, several satellites were set to "Unusable" for short periods of time. A complete list of Galileo NAGUs is available in Table 7-2.

Table 3-2. Galileo Satellite Data: 1st Quarter 2023

Data Evaluation	Number of Samples	Percentage of Total
Valid Data Evaluation	573501	98.046%
No Evaluation due to SV Unhealthy/Marginal	11362	1.942%
No Evaluation due to Exceeding 4-hour Fit Interval	25	0.004%
No Evaluation due to Precise Data Event Flag	40	0.007%
Faults	0	0.000%

3.4   Data Partitioning

Performance is analyzed and presented using several data partitions to show various dependencies. These include time, the individual satellite, the satellite block type, the broadcast URA/SISA value, or combinations of these.

See Table 3-3 for this quarter's current PRN assignments for GPS satellites. See Table 3-4 for this quarter's current SVID assignments for Galileo satellites. Auxiliary satellites SVID10 (GSAT0224), SVID14 (GSAT0202), and SVID18 (GSAT0201) are not evaluated in this report.

Table 3-3. GPS PRN Assignment by SVN

PRN	SVN	Block Type
1	63	IIF
2	61	IIR
3	69	IIF
4	74	III
5	50	IIR-M
6	67	IIF
7	48	IIR-M
8	72	IIF
9	68	IIF
10	73	IIF
11	78	III
12	58	IIR-M
13	43	IIR
14	77	III
15	55	IIR-M
16	56	IIR
17	53	IIR-M
18	75	III
19	59	IIR
20	51	IIR
21	45	IIR
22	41	IIR
23	76	III
24	65	IIF
25	62	IIF
26	71	IIF
27	66	IIF
28	79	III
29	57	IIR-M
30	64	IIF
31	52	IIR-M
32	70	IIF

Table 3-4. Galileo SVID Assignment by Satellite Name

SVID	Name	Block
1	GSAT0210	FOC 1
2	GSAT0211	FOC 1
3	GSAT0212	FOC 1
4	GSAT0213	FOC 1
5	GSAT0214	FOC 1
7	GSAT0207	FOC 1
8	GSAT0208	FOC 1
9	GSAT0209	FOC 1
11	GSAT0101	IOV
12	GSAT0102	IOV
13	GSAT0220	FOC 2
15	GSAT0221	FOC 2
19	GSAT0103	IOV
21	GSAT0215	FOC 2
22	GSAT0204	FOC 1
24	GSAT0205	FOC 1
25	GSAT0216	FOC 2
26	GSAT0203	FOC 1
27	GSAT0217	FOC 2
30	GSAT0206	FOC 1
31	GSAT0218	FOC 2
33	GSAT0222	FOC 2
34	GSAT0223	FOC 3
36	GSAT0219	FOC 2

4.   DATA LIMITATIONS

GPS SIS anomalies are listed in Table 7-1 and Galileo SIS anomalies are listed in Table 7-2. There are some limitations of SIS anomaly reporting due to potential errors in the source data or missing source data. Some limitations include:

- False SIS anomalies may be reported due to errors in the precise ephemerides/clock or errors in the validated navigation messages.
- Short-duration SIS anomalies may not be reported if they happen to fall within the 5- or 15-minute gaps of the precise ephemerides/clocks.

- True SIS anomalies may not be detected if the precise ephemerides/clocks, or LNAV/FNAV data, are temporarily missing or incorrect, for any reason.

4.1 Data Analysis

The goal of the data analysis process is to determine whether the behavior of the observed data is consistent with the underlying assumptions and the CSP commitments.

The first step in the process is to remove, as completely as possible, any errors that have been introduced by the data collection process itself. These include transmission errors, incomplete data sets from an individual source, conflicting data from separate sources, or any other known error type.

The next step is the nominal performance analysis, to ensure that the nominal observed error distributions are Gaussian and bounded by the URA, as defined in the SPS PS and OS SDD. The error characteristic is observed in the probability density function (PDF) plots of the RAC, clock, and SISE errors.

A sigma overbounding and the ratio of the minimum overbounding sigma to the broadcast URA and the Gaussian curve are computed. A PDF of SISEs is used to observe the core of the error distribution, and a cumulative distribution function (CDF) is used to observe the tail behavior.

Correlation of errors is also checked to ensure that the individual ranging errors do not combine to form unexpectedly large position errors. The sum of the squares of the URA-normalized residuals is computed for each time step and user, and all samples are combined in a single distribution. Correlated residuals will be indicated by a sum of square residuals distribution that exceeds a chi-square distribution.

After the signal performance analysis, any potential faults are analyzed. That analysis will provide, at a minimum, the date, time, and duration of the fault, as well as the overall effect on fault rates and probabilities. A description of the potential fault will be provided, as well as the basis used to identify it. If possible, the initial cause of the fault will also be determined and described, along with any associated maintenance action taken.

The data in this report is presented using different views and data partitions to describe performance more completely. The different types of views include statistical plots, such as probability, residual error over time, histograms, one minus CDF (1-CDF) plots, and data tables, partitioned by satellite, block types, and composite. These views show: overbounding of the measured data by the integrity parameters, comparison of residuals (based on an independent reference) of orbital and clock parameters, presentation of range error in different units and coordinate systems, projected user errors, and comparison to historical performance.

5. NOMINAL ACCURACY AND URA BOUNDING

GPS satellites broadcast URA values to indicate the expected level of accuracy. The broadcast URA is equivalent to the σ_{URA} ISM term. Galileo satellites broadcast SISA to indicate the expected level of accuracy. A separate bounding term (σ_{URA}) will be provided in the Galileo ARAIM ISM

as the URA overbound term. SISA is evaluated in this section as an estimate to the constellation's accuracy only. For normalization and overbound analysis, the maximum single frequency σ_{URA} of 7.5 m is used for Galileo. This is subject to change as the Galileo broadcast ISM becomes available.

The URA (σ_{URA}) represents a 1-sigma value that conservatively characterizes the nominal signal accuracy. Offline monitoring of the URA parameter assesses the integrity of the ephemeris and clock data in the broadcast navigation messages, by evaluating the URA bounding performance of nominal, fault-free range errors. The observed error distributions are examined to evaluate how well the URA describes them.

5.1   Broadcast URA/SISA

Broadcast URA values are shown in Figure 5-1 and Table 5-1 for GPS data from January 1, 2008 to March 31, 2023, and Figure 5-2 and Table 5-2 for the 1st Quarter 2023. Broadcast SISA values are shown in Figure 5-3 and Table 5-3 for Galileo data from January 1, 2020 to March 31, 2023, and Figure 5-4 and Table 5-4 for the 1st Quarter 2023. The figures and tables show the relative frequency of different broadcast values by satellite and block type for each constellation.

The URA index of 1 (corresponding to 2.4 m) is the most common URA value since January 1, 2008. This value was sent 93.673% of the time for all satellites. The next most common index value of 2 (corresponding to 3.4 m) was sent 5.914% of the time. Both values combined accounted for 99.587% of all broadcast URA.

For this quarter, the URA value of 2.4 m was sent 92.752% of the time, and 3.4 m was sent 5.656% of the time. Both values combined accounted for 98.408% of all broadcast URA.

The SISA index of 107, corresponding to 3.12 m, is the most common SISA value since January 1, 2020. This value was sent 99.424% of the time for all satellites. The next most common index value of 110, corresponding to 3.6 m, was sent 0.361% of the time. Both values combined accounted for 99.785% of all broadcast SISA.

For this quarter, the SISA value of 3.12 m was sent 99.829% of the time, and 3.4 m was sent 0.055% of the time. Both values combined accounted for 99.884% of all broadcast SISA.

A SISA index of 255 represents No Accuracy Prediction Available (NAPA) and indicates the satellite is in a marginal state. A marginal broadcast is included in the count with unhealthy satellites and is not tracked individually.
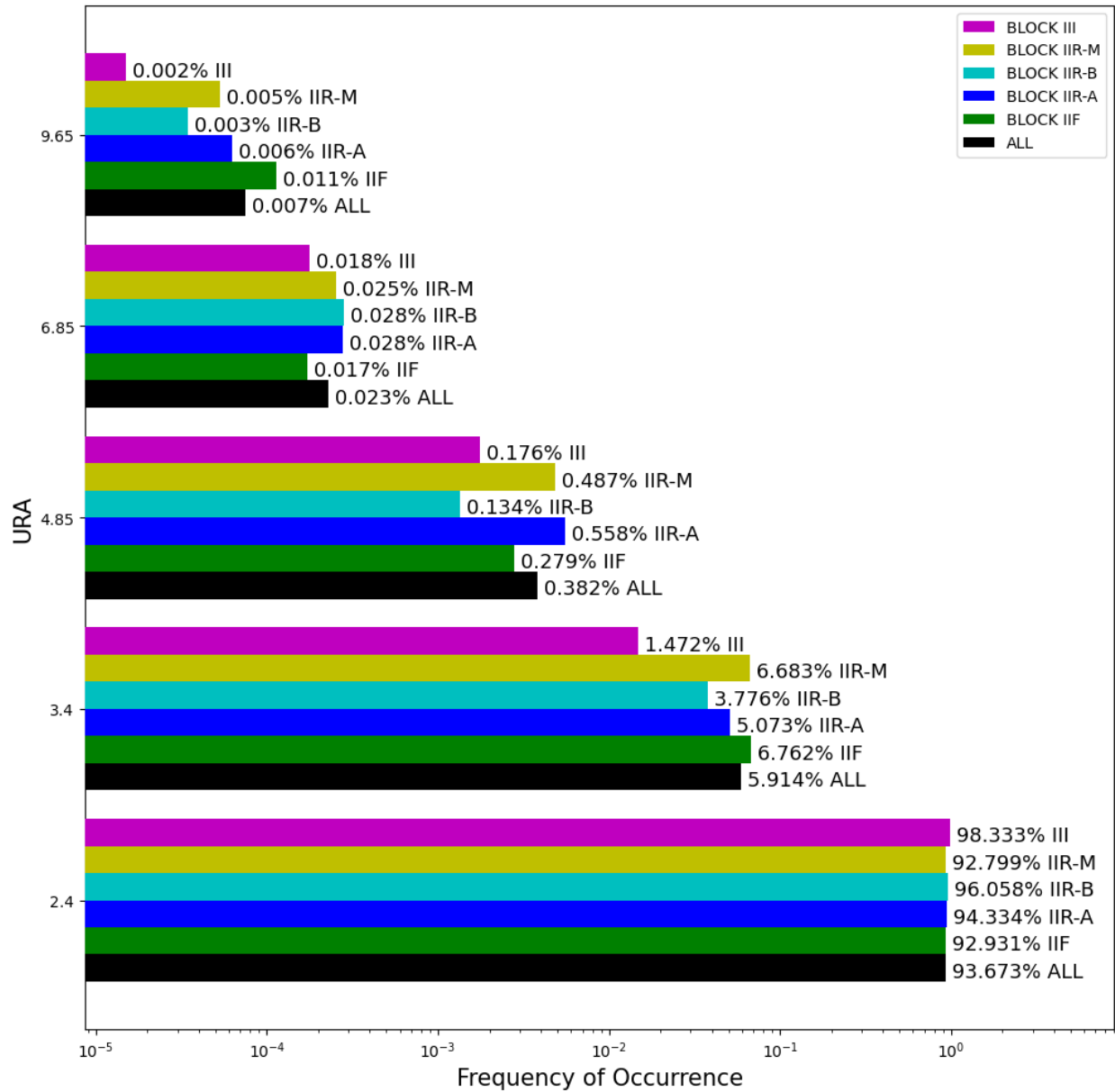
Figure 5-1. GPS Relative Frequency of URA: January 1, 2008 to March 31, 2023

Table 5-1. GPS Relative Frequency of URA: January 1, 2008 to March 31, 2023

	2.4	3.4	4.85	6.85	9.65
ALL	93.673	5.914	0.382	0.023	0.007
BLOCK IIF	92.931	6.762	0.279	0.017	0.011
BLOCK IIR-A	94.334	5.073	0.558	0.028	0.006
BLOCK IIR-B	96.058	3.776	0.134	0.028	0.003
BLOCK IIR-M	92.799	6.683	0.487	0.025	0.005
BLOCK III	98.333	1.472	0.176	0.018	0.002
43	95.044	4.890	0.048	0.009	0.007
41	92.869	6.840	0.234	0.041	0.015
45	92.384	6.390	1.191	0.035	0.000
48	93.521	5.250	1.150	0.076	0.003
50	98.081	1.845	0.056	0.009	0.007
51	95.014	3.722	1.226	0.033	0.005
52	94.242	5.398	0.323	0.025	0.012
53	83.885	15.115	0.977	0.011	0.009
55	96.788	3.162	0.036	0.015	N/A
56	96.155	3.770	0.048	0.023	0.004
57	88.597	11.311	0.074	0.011	0.007
58	94.720	4.475	0.775	0.030	N/A
59	96.872	3.061	0.034	0.029	0.005
61	95.242	4.492	0.235	0.028	0.002
62	95.927	3.983	0.070	0.016	0.004
63	94.528	5.323	0.131	0.008	0.009
64	95.228	4.701	0.054	0.017	N/A
65	77.251	22.298	0.434	0.016	0.001
66	94.842	5.023	0.130	0.005	N/A
67	97.540	2.370	0.047	0.025	0.018
68	97.175	2.750	0.047	0.015	0.013
69	88.333	9.537	2.055	0.043	0.032
70	96.594	3.264	0.072	0.028	0.042
71	95.147	4.774	0.037	0.017	0.024
72	87.689	12.108	0.177	0.021	0.006
73	96.847	2.954	0.200	N/A	N/A
74	99.212	0.657	0.104	0.023	0.004
75	98.384	1.500	0.068	0.046	0.002
76	98.286	1.490	0.223	N/A	N/A
77	97.691	2.032	0.277	N/A	N/A
78	99.012	0.988	N/A	N/A	N/A
79	81.900	14.960	3.140	N/A	N/A
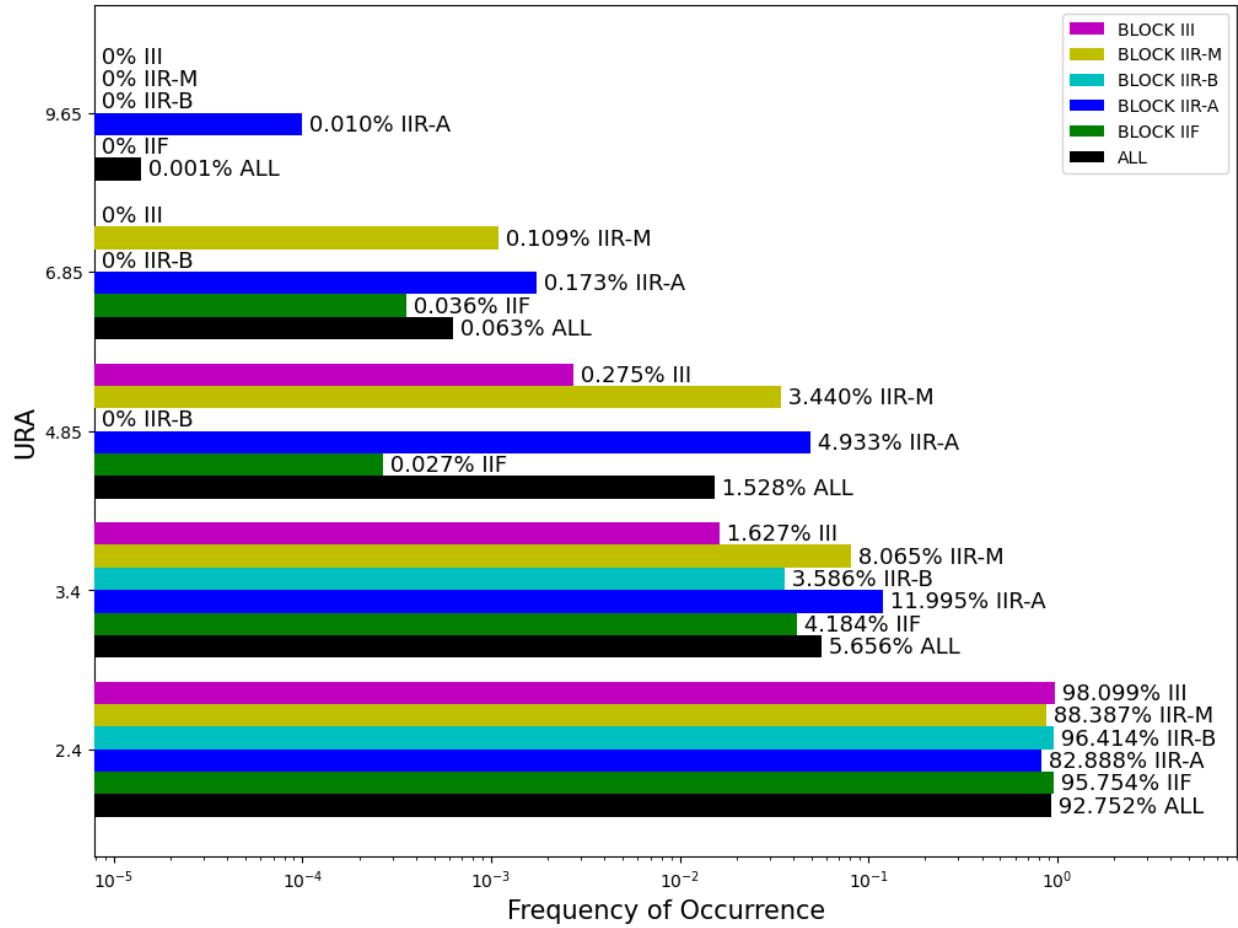
Figure 5-2. GPS Relative Frequency of URA: 1st Quarter 2023

Table 5-2. GPS Relative Frequency of URA: 1st Quarter 2023

	2.4	3.4	4.85	6.85	9.65
ALL	92.752	5.656	1.528	0.063	0.001
BLOCK IIF	95.754	4.184	0.027	0.036	N/A
BLOCK IIR-A	82.888	11.995	4.933	0.173	0.010
BLOCK IIR-B	96.414	3.586	N/A	N/A	N/A
BLOCK IIR-M	88.387	8.065	3.440	0.109	N/A
BLOCK III	98.099	1.627	0.275	N/A	N/A
43	87.913	12.087	N/A	N/A	N/A
41	94.824	2.227	0.568	2.212	0.169
45	82.315	14.425	3.261	N/A	N/A
48	98.220	1.045	0.368	0.368	N/A
50	98.827	1.173	N/A	N/A	N/A
51	62.739	19.738	17.342	0.181	N/A
52	98.470	1.530	N/A	N/A	N/A
53	86.053	13.947	N/A	N/A	N/A
55	99.649	0.351	N/A	N/A	N/A
56	95.621	4.166	0.213	N/A	N/A
57	88.175	11.825	N/A	N/A	N/A
58	49.383	26.535	23.688	0.394	N/A
59	96.755	3.245	N/A	N/A	N/A
61	96.073	3.927	N/A	N/A	N/A
62	94.453	5.029	0.093	0.426	N/A
63	96.999	3.001	N/A	N/A	N/A
64	97.539	2.461	N/A	N/A	N/A
65	98.032	1.968	N/A	N/A	N/A
66	91.821	8.179	N/A	N/A	N/A
67	95.818	4.182	N/A	N/A	N/A
68	99.726	0.274	N/A	N/A	N/A
69	89.796	9.977	0.228	N/A	N/A
70	99.209	0.791	N/A	N/A	N/A
71	95.745	4.255	N/A	N/A	N/A
72	94.958	5.042	N/A	N/A	N/A
73	95.038	4.962	N/A	N/A	N/A
74	99.549	0.451	N/A	N/A	N/A
75	99.410	0.590	N/A	N/A	N/A
76	99.576	0.424	N/A	N/A	N/A
77	99.884	0.116	N/A	N/A	N/A
78	99.838	0.162	N/A	N/A	N/A
79	81.900	14.960	3.140	N/A	N/A
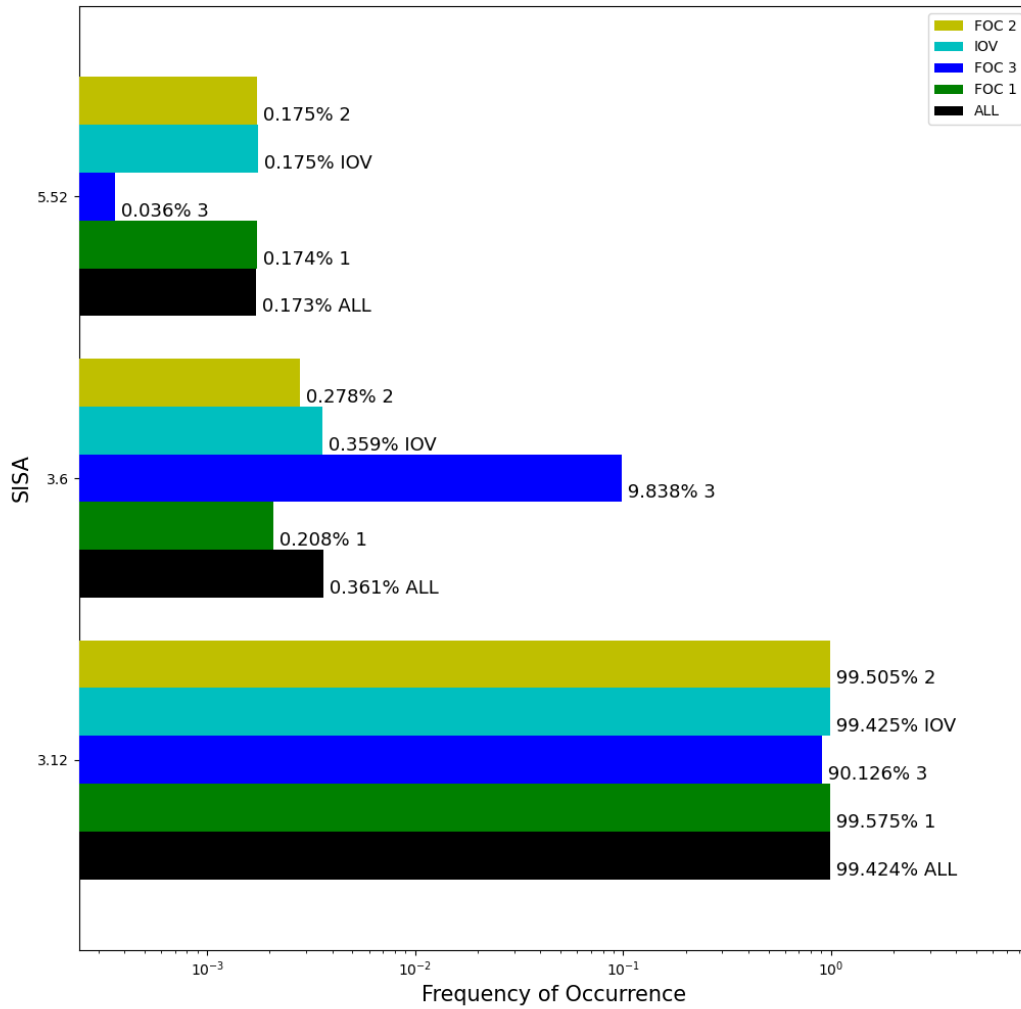
**Figure 5-3. Galileo Relative Frequency of SISA: January 1, 2020 to March 31, 2023**

Table 5-3. Galileo Relative Frequency of SISA: January 1, 2020 to March 31, 2023

Block/GSAT	3.12	3.6	5.52
ALL	99.424	0.361	0.173
IOV	99.425	0.359	0.175
FOC 1	99.575	0.208	0.174
FOC 3	90.126	9.838	0.036
FOC 2	99.505	0.278	0.175
102	99.709	0.079	0.170
101	98.921	0.856	0.171
103	99.659	0.131	0.185
203	99.353	0.429	0.169
205	99.782	0.009	0.170
206	99.739	0.038	0.174
207	99.781	0.010	0.172
208	99.772	0.002	0.173
209	99.779	0.009	0.173
210	99.012	0.740	0.194
211	98.659	1.121	0.175
212	99.792	N/A	0.174
213	99.786	0.008	0.168
214	99.791	N/A	0.169
215	97.618	2.158	0.175
216	99.772	N/A	0.179
217	99.782	0.007	0.173
218	99.779	0.002	0.172
219	99.733	0.061	0.176
220	99.776	0.004	0.175
221	99.780	0.005	0.172
222	99.787	N/A	0.175
223	90.126	9.838	0.036
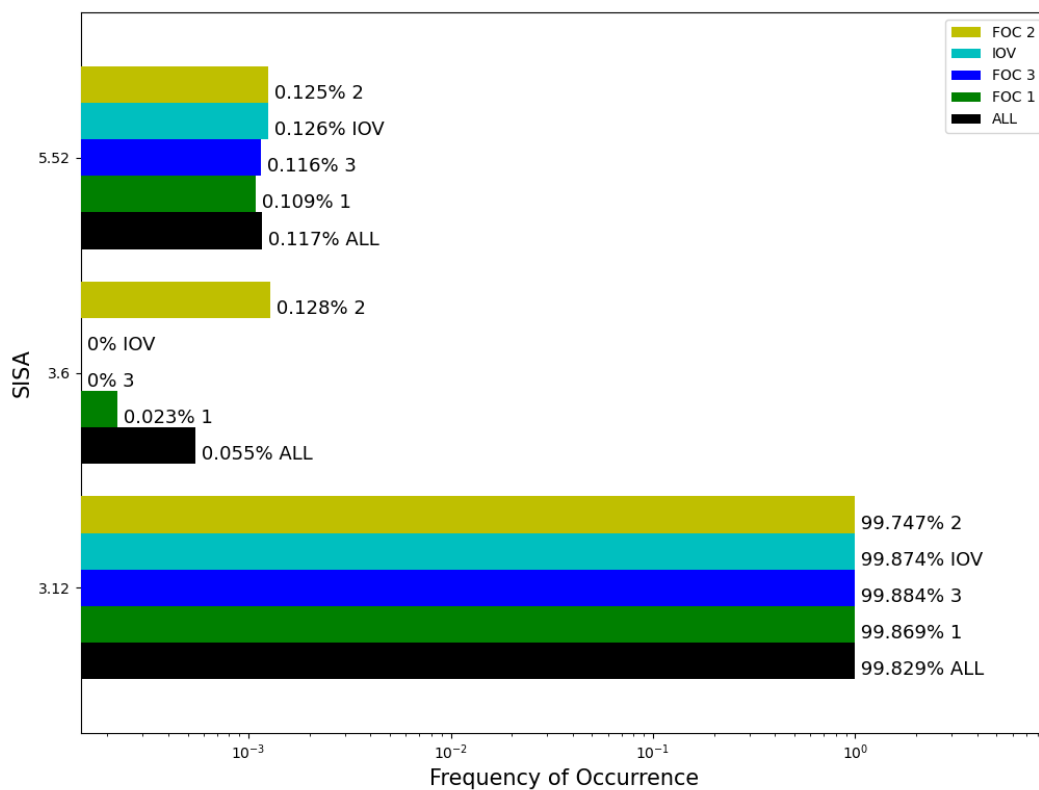
Figure 5-4. Galileo Relative Frequency of SISA: 1st Quarter 2023

Table 5-4. Galileo Relative Frequency of SISA: 1st Quarter 2023

Block/GSAT	3.12	3.6	5.52
ALL	99.829	0.055	0.117
IOV	99.874	N/A	0.126
FOC 1	99.869	0.023	0.109
FOC 3	99.884	N/A	0.116
FOC 2	99.747	0.128	0.125
102	99.846	N/A	0.154
101	99.892	N/A	0.108
103	99.884	N/A	0.116
203	99.789	0.089	0.122
205	99.885	N/A	0.115
206	99.792	0.083	0.125
207	99.884	N/A	0.116
208	99.884	N/A	0.116
209	99.884	N/A	0.116
210	99.905	0.095	N/A
211	99.884	N/A	0.116
212	99.884	N/A	0.116
213	99.879	N/A	0.121
214	99.884	N/A	0.116
215	99.896	N/A	0.104
216	99.884	N/A	0.116
217	99.768	0.098	0.134
218	99.877	N/A	0.123
219	99.046	0.832	0.122
220	99.837	0.032	0.131
221	99.777	0.069	0.154
222	99.882	N/A	0.118
223	99.884	N/A	0.116

5.2   Accuracy

Orbit, clock, and projected range errors are shown in this section for the current quarter. The errors consist of RAC, clock, and the aggregated UPE across 200 user locations, for the quarter. Table 5-5 shows the mean, 68%, and 95% values for GPS RAC, clock, and UPE errors by satellite, block type, and the aggregated total. The maximum UPE mean was -0.314 m on SVN64, the maximum UPE 68% value was 0.960 m on SVN72, and the maximum UPE 95% was 2.240 m on SVN72.

Table **5-6** shows the mean, 68%, and 95% values for Galileo RAC, clock, and UPE errors by satellite, block type, and the aggregated total. The maximum UPE mean was -0.958 m on GSAT0215, the maximum UPE 68% value was 1.00 m on GSAT0215, and the maximum UPE 95% was 1.140 m on GSAT0215.

Figure 5-5 shows the RAC, clock, and UPE errors for GPS, and Figure 5-7 shows the RAC, clock, and UPE errors for Galileo. The green segment represents the (68%) area of the error distribution, and the upper and lower fences represent the (95%) area of the error distribution. The center tick value is the mean of the nominal error distribution. The scale for each parameter is adjusted to focus on the range of most interest.

Figure 5-6 shows the aggregated PDF of the GPS errors, and Figure 5-8 shows the Galileo aggregated PDF. For this quarter, most errors appeared nearly Gaussian for both GPS and Galileo; radial errors were the smallest, and along-track errors were the largest. The aggregated UPE across 200 user locations align closely with the clock errors.

Table 5-5. GPS RAC, Clock, and UPE Errors: 1st Quarter 2023

SVN	Block	Along-Track			Clock			Cross-Track			Radial			User Projected Error		
		mean	68%	95%	mean	68%	95%	mean	68%	95%	mean	68%	95%	mean	68%	95%
41	BLOCK IIR-A	0.309	0.880	1.880	0.023	0.320	0.640	0.064	0.520	1.040	-0.010	0.160	0.320	-0.033	0.360	0.700
43		-0.248	0.840	1.760	0.077	0.400	0.880	-0.043	0.480	0.960	0.021	0.160	0.280	-0.057	0.420	0.900
45		0.025	1.200	2.520	-0.096	0.320	0.760	-0.015	0.520	1.160	-0.017	0.200	0.360	0.079	0.380	0.860
51		-0.216	0.880	1.800	-0.014	0.320	0.680	-0.004	0.440	0.880	0.013	0.120	0.240	0.027	0.340	0.760
56		0.357	0.920	1.920	0.089	0.280	0.520	0.027	0.600	1.120	-0.027	0.160	0.280	-0.116	0.300	0.600
59	BLOCK IIR-B	0.446	0.840	1.920	-0.017	0.240	0.480	0.029	0.400	0.840	-0.002	0.160	0.280	0.015	0.280	0.580
61		0.466	0.920	2.000	-0.035	0.280	0.560	-0.045	0.480	1.000	-0.017	0.160	0.280	0.018	0.320	0.640
48	BLOCK IIR-M	0.014	0.880	1.920	0.052	0.440	0.920	0.033	0.920	1.680	0.020	0.200	0.320	-0.032	0.460	1.020
50		0.165	0.880	1.640	0.016	0.240	0.440	-0.083	0.440	0.880	-0.005	0.240	0.360	-0.021	0.260	0.520
52		0.640	1.160	2.200	0.062	0.400	0.840	-0.018	0.480	0.960	-0.021	0.160	0.280	-0.084	0.420	0.920
53		-0.082	1.000	2.120	-0.005	0.520	1.520	0.044	0.480	1.080	0.012	0.200	0.320	0.017	0.560	1.520
55		0.033	0.680	1.400	0.033	0.240	0.440	-0.045	0.480	0.920	0.004	0.160	0.280	-0.029	0.240	0.540
57		0.161	0.720	1.440	-0.065	0.400	1.200	0.046	0.400	0.760	0.004	0.160	0.320	0.069	0.400	1.180
58		-0.488	1.000	2.160	-0.178	0.360	0.800	0.038	0.520	1.080	0.066	0.160	0.280	0.243	0.420	0.880
62	BLOCK IIF	-0.032	0.800	1.760	-0.075	0.400	0.640	0.020	0.560	1.280	0.004	0.160	0.280	0.079	0.420	0.720
63		0.173	0.680	1.480	0.026	0.200	0.400	-0.074	0.480	0.920	-0.002	0.200	0.360	-0.028	0.300	0.580
64		0.700	1.000	2.120	0.270	0.440	0.720	0.050	0.600	1.200	-0.045	0.160	0.320	-0.314	0.480	0.880
65		0.867	1.320	2.840	0.127	0.280	0.480	0.029	0.440	1.040	-0.051	0.200	0.400	-0.176	0.380	0.840
66		0.441	0.880	2.000	-0.024	0.280	0.640	-0.054	0.440	0.880	-0.013	0.200	0.360	0.011	0.380	0.800
67		0.181	0.680	1.600	0.093	0.240	0.480	-0.050	0.400	0.800	0.008	0.160	0.280	-0.084	0.300	0.580
68		0.406	0.880	1.880	-0.119	0.240	0.480	0.026	0.400	0.840	-0.007	0.240	0.400	0.112	0.340	0.640
69		0.116	0.880	1.880	0.101	0.520	1.360	0.045	0.480	1.040	0.009	0.240	0.400	-0.092	0.520	1.400
70		-0.427	0.840	1.880	-0.036	0.240	0.440	0.002	0.720	1.360	0.039	0.240	0.400	0.074	0.340	0.720
71		-0.167	0.840	1.800	0.070	0.240	0.440	-0.011	0.520	1.000	0.026	0.160	0.280	-0.044	0.280	0.560
72		0.056	0.920	2.080	-0.119	0.960	2.160	-0.081	0.480	1.040	0.000	0.240	0.520	0.120	0.960	2.240
73		0.218	0.840	1.840	-0.143	0.920	2.040	-0.046	0.560	1.120	0.012	0.200	0.400	0.155	0.940	2.080

SVN	Block	Along-Track			Clock			Cross-Track			Radial			User Projected Error		
		mean	68%	95%	mean	68%	95%	mean	68%	95%	mean	68%	95%	mean	68%	95%
74	BLOCK III	-0.064	0.960	1.760	0.016	0.200	0.400	-0.003	0.600	1.280	0.015	0.120	0.240	-0.001	0.260	0.500
75		-0.338	0.760	1.680	-0.029	0.200	0.360	-0.013	0.720	1.320	0.042	0.160	0.320	0.070	0.300	0.580
76		-0.632	1.160	2.400	0.019	0.200	0.360	-0.092	0.520	1.160	0.049	0.200	0.320	0.029	0.300	0.600
77		-0.068	0.880	1.840	0.016	0.200	0.360	0.015	0.520	1.000	0.001	0.120	0.200	-0.016	0.240	0.480
78		0.269	0.760	1.440	-0.034	0.200	0.360	-0.019	0.400	0.760	0.007	0.160	0.280	0.040	0.260	0.520
79		-0.655	1.520	3.640	-0.159	0.280	0.720	-0.063	0.640	1.480	0.046	0.200	0.400	0.205	0.400	0.980

Table 5-6. Galileo RAC, Clock, and UPE Errors: 1st Quarter 2023

GSAT	Block	Along-Track			Clock			Cross-Track			Radial			User Projected Error		
		mean	68%	95%	mean	68%	95%	mean	68%	95%	mean	68%	95%	mean	68%	95%
101	IOV	0.465	0.600	1.160	0.039	0.200	0.400	-0.033	0.320	0.640	-0.206	0.280	0.440	-0.242	0.300	0.500
102	IOV	0.328	0.480	1.080	-0.131	0.240	0.440	-0.022	0.280	0.600	-0.279	0.360	0.520	-0.143	0.220	0.420
103	IOV	0.215	0.440	0.840	-0.004	0.240	0.440	-0.014	0.280	0.520	-0.195	0.280	0.480	-0.187	0.260	0.460
203	FOC 1	0.321	0.440	0.960	0.015	0.200	0.360	-0.103	0.280	0.560	0.144	0.240	0.360	0.126	0.180	0.300
205	FOC 1	0.370	0.480	1.040	-0.005	0.120	0.240	0.126	0.320	0.640	0.235	0.280	0.400	0.236	0.300	0.420
206	FOC 1	0.293	0.400	0.840	-0.026	0.120	0.280	0.141	0.320	0.560	0.274	0.320	0.440	0.296	0.360	0.460
207	FOC 1	0.273	0.400	0.880	0.011	0.160	0.320	0.007	0.240	0.520	0.282	0.360	0.520	0.267	0.320	0.440
208	FOC 1	0.281	0.400	0.840	-0.028	0.200	0.320	0.010	0.280	0.520	0.200	0.280	0.440	0.224	0.280	0.400
209	FOC 1	0.315	0.440	0.920	0.003	0.160	0.320	0.027	0.280	0.600	0.217	0.320	0.440	0.211	0.260	0.380
210	FOC 1	0.316	0.440	0.960	0.007	0.160	0.280	0.107	0.280	0.560	0.240	0.320	0.400	0.233	0.300	0.440
211	FOC 1	0.339	0.480	1.000	-0.023	0.120	0.240	0.128	0.320	0.600	0.210	0.280	0.400	0.230	0.280	0.400
212	FOC 1	0.323	0.440	0.960	-0.021	0.200	0.320	0.007	0.280	0.560	0.173	0.280	0.400	0.191	0.260	0.380
213	FOC 1	0.353	0.480	1.040	-0.003	0.200	0.320	0.012	0.320	0.640	0.178	0.280	0.400	0.178	0.240	0.360
214	FOC 1	0.346	0.440	1.000	-0.005	0.200	0.320	0.006	0.280	0.600	0.123	0.200	0.360	0.126	0.180	0.320
215	FOC 2	0.346	0.480	0.960	0.040	0.120	0.240	-0.046	0.240	0.520	-0.932	1.000	1.080	-0.958	1.000	1.140
216	FOC 2	0.437	0.560	1.120	0.015	0.120	0.240	-0.022	0.320	0.640	-0.822	0.880	1.000	-0.824	0.880	1.020
217	FOC 2	0.310	0.440	0.880	0.029	0.120	0.240	-0.029	0.240	0.520	-0.807	0.880	0.960	-0.823	0.880	1.000

| GSAT	Block	Along-Track			Clock			Cross-Track			Radial			User Projected Error		
		mean	68%	95%	mean	68%	95%	mean	68%	95%	mean	68%	95%	mean	68%	95%
218	FOC 2	0.357	0.480	1.040	0.009	0.120	0.240	-0.027	0.280	0.600	-0.819	0.880	1.000	-0.815	0.860	1.000
219	FOC 2	0.446	0.600	1.160	0.048	0.200	0.320	0.015	0.320	0.680	-0.793	0.880	1.040	-0.828	0.880	1.040
220	FOC 2	0.342	0.480	1.040	-0.025	0.200	0.360	-0.007	0.280	0.560	-0.891	0.960	1.120	-0.852	0.920	1.080
221	FOC 2	0.353	0.480	1.040	0.003	0.200	0.320	-0.002	0.280	0.600	-0.802	0.880	1.040	-0.792	0.840	1.000
222	FOC 2	0.364	0.480	1.120	-0.008	0.160	0.320	-0.005	0.280	0.600	-0.824	0.920	1.040	-0.803	0.860	1.000
223	FOC 3	0.381	0.520	1.080	0.028	0.200	0.320	0.004	0.280	0.600	-0.812	0.880	1.040	-0.827	0.880	1.020
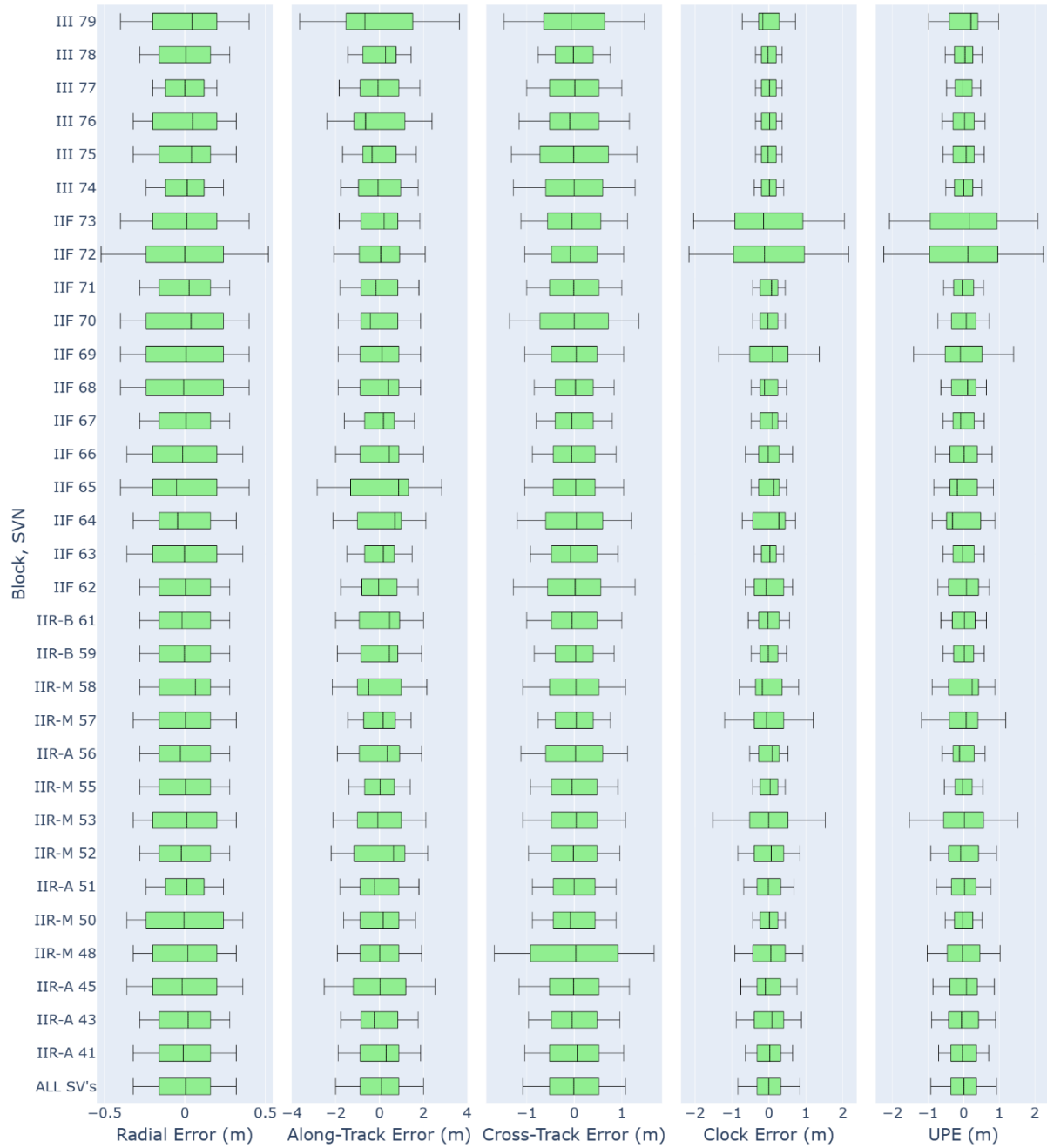
Figure 5-5. GPS RAC, Clock, and UPE Errors Box Plot: 1st Quarter 2023
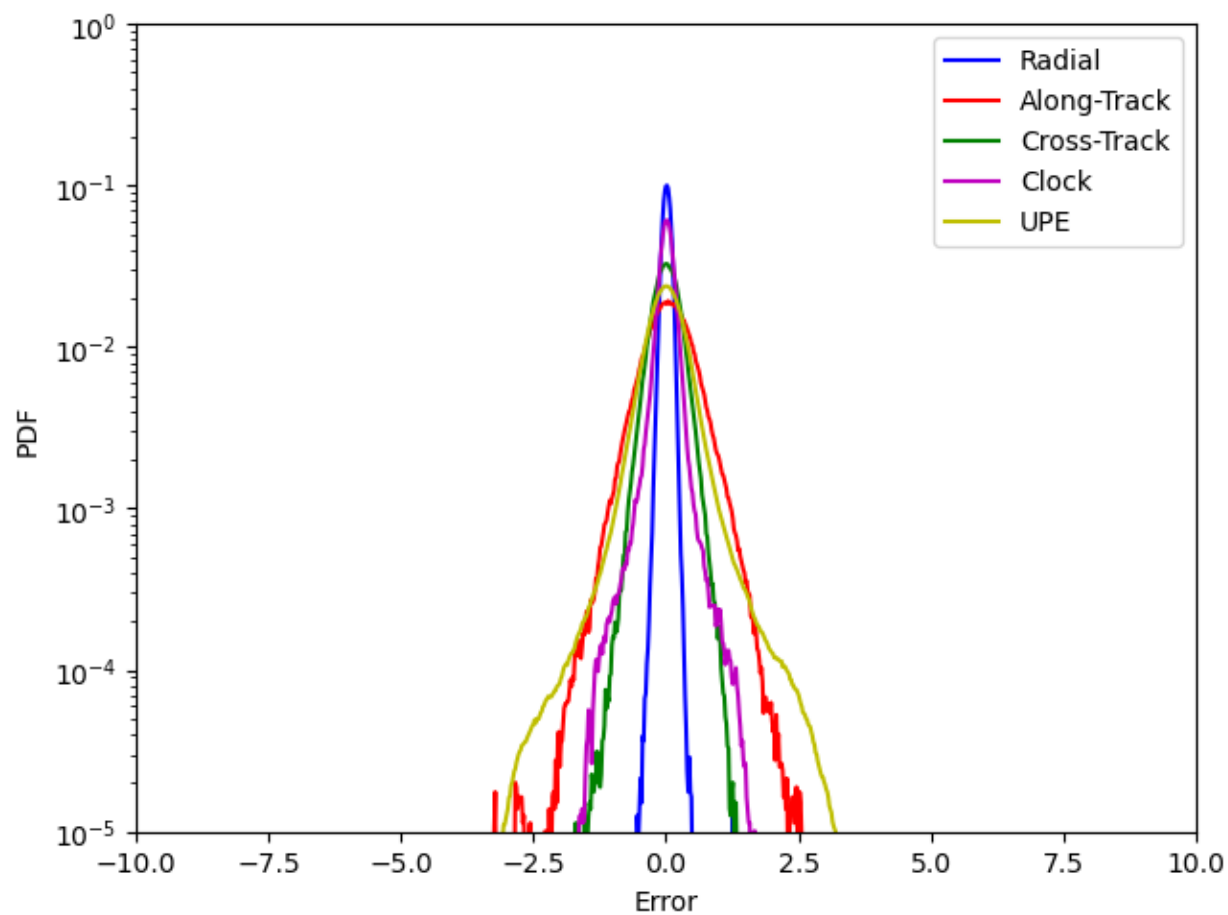
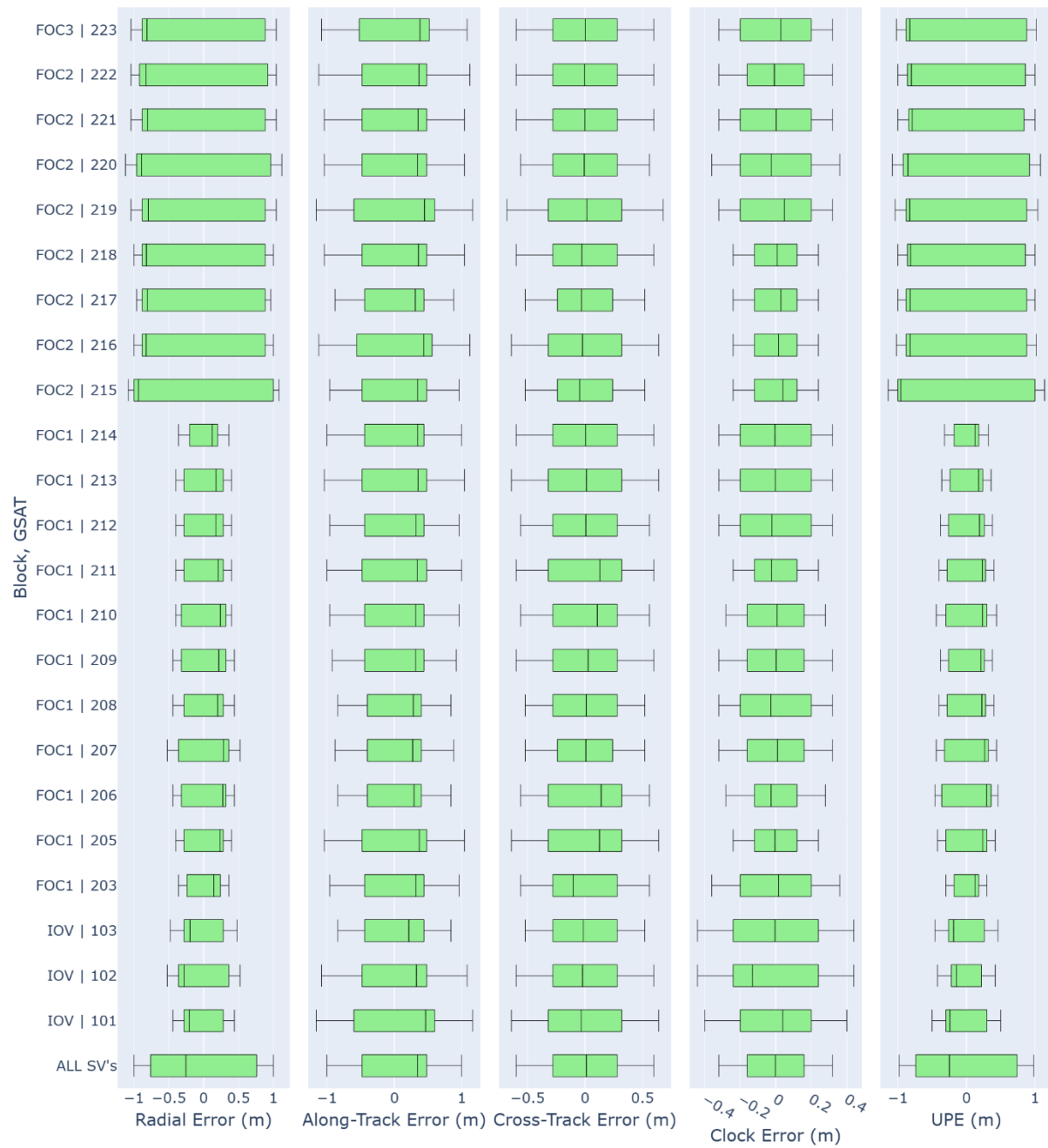**Figure 5-6. GPS RAC, Clock, and UPE Errors (PDF): 1st Quarter 2023**

Figure 5-7. Galileo RAC, Clock, and UPE Errors Box Plot: 1st Quarter 2023
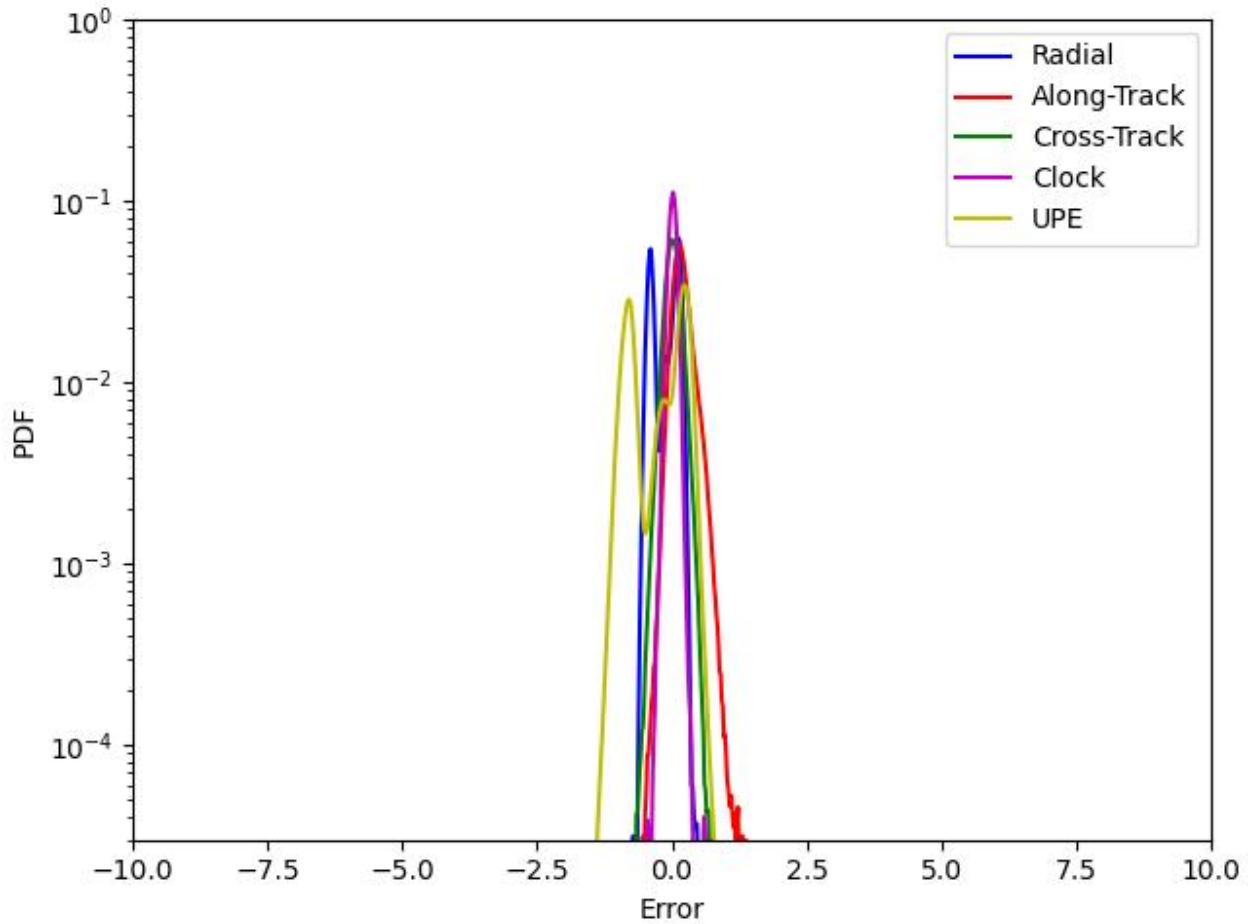
Figure 5-8. Galileo RAC, Clock, and SISE Errors (PDF): 1st Quarter 2023

GPS historical performance data are presented by satellite for all available data since January 1, 2008. Galileo historical performance data are presented by satellite for all available data since January 1, 2020. GPS monthly mean SISE errors are shown in Figure 5-9. The monthly 95% error bounds are shown in Figure 5-10. Galileo monthly mean SISE errors are shown in Figure 5-11. The monthly 95% error bounds are shown in Figure 5-12. Table 5-7 and Table 5-8 show the absolute value of the minimum and maximum of the monthly means and 95% values for GPS and Galileo, respectively.

All monthly means for GPS satellites were under 0.95 m with the high value of 0.904 m on SVN63accepted, and all monthly 95% values were under 2.8 m with the high value of 2.780 m on SVN48. All monthly means for Galileo satellites were under 1.00 m with the high value of 0.987 m on GSAT0215, and all monthly 95% values were under 1.3 m with the high value of 1.200 m on GSAT0215.
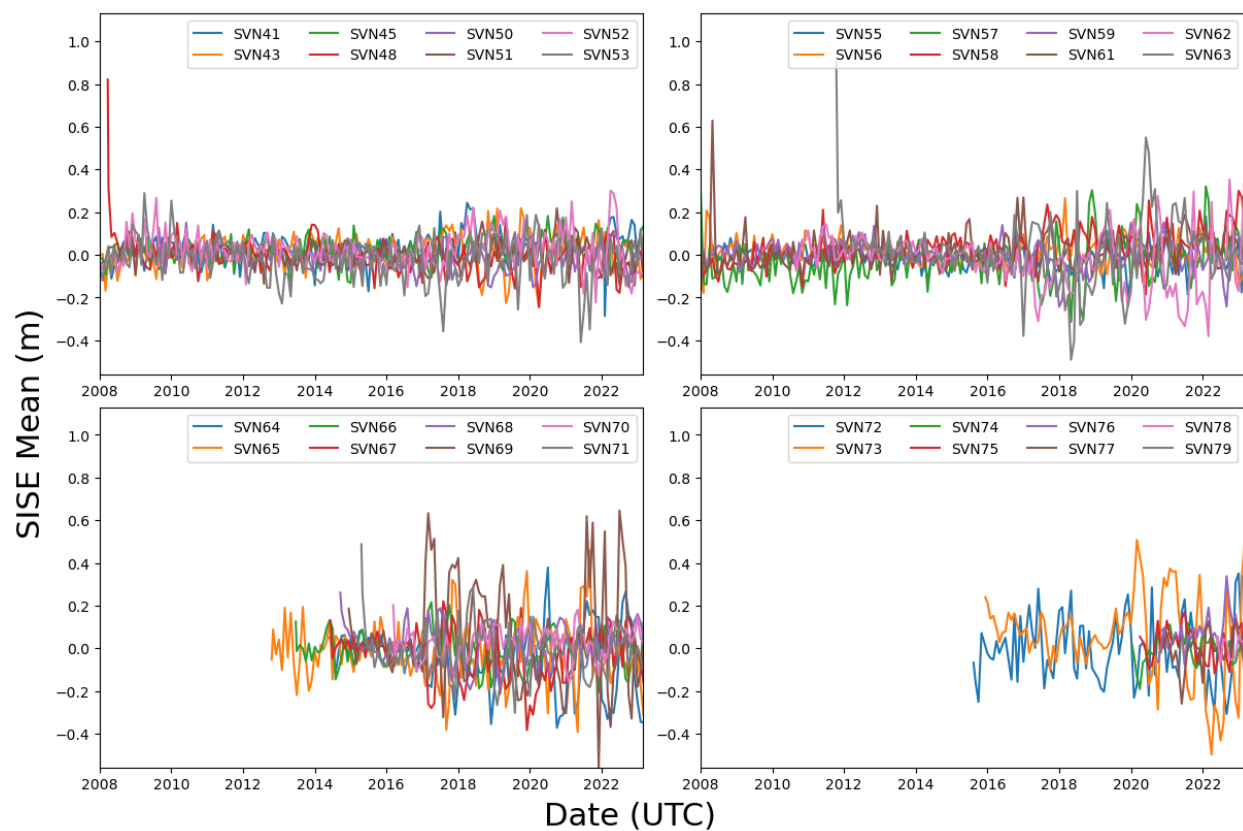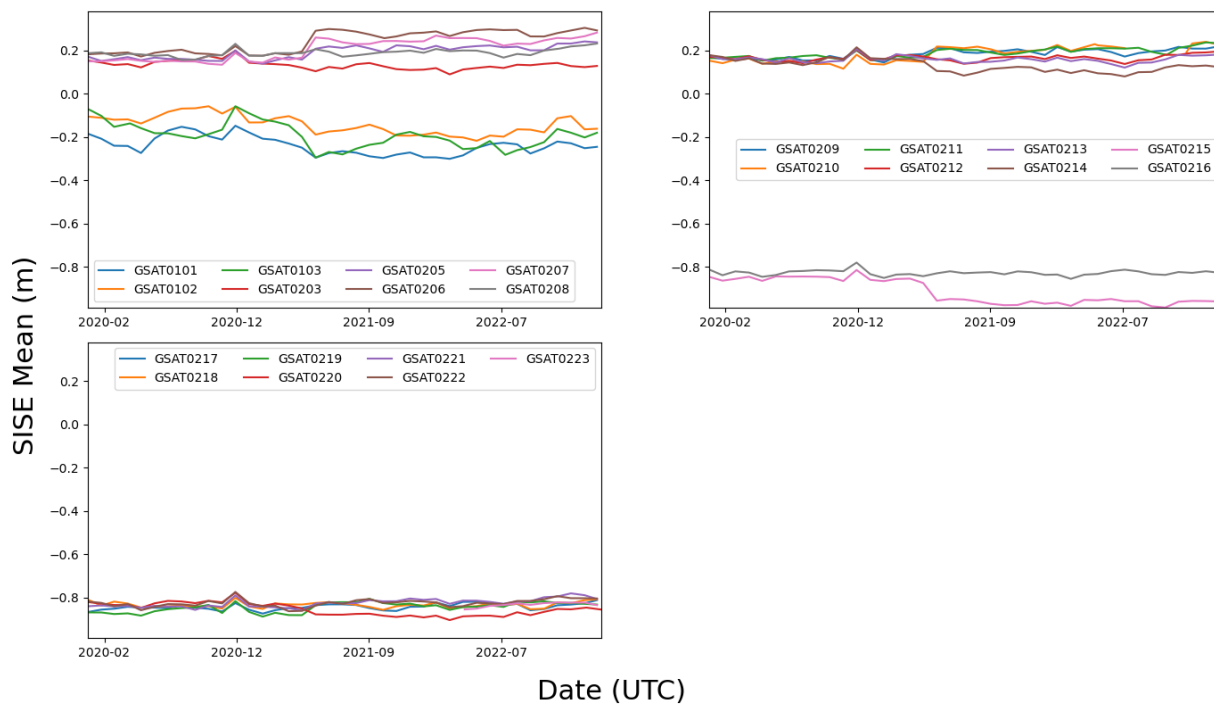
Figure 5-9. GPS Monthly Mean SISE:
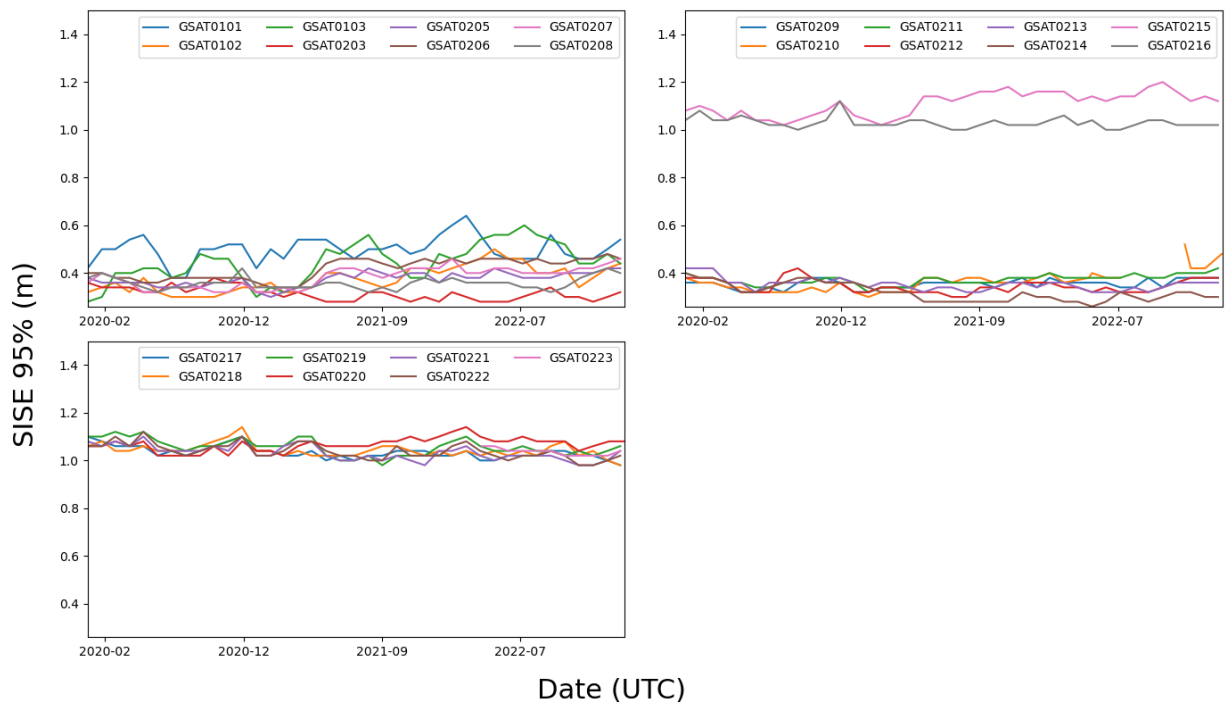**January 1, 2008 to March 31, 2023**
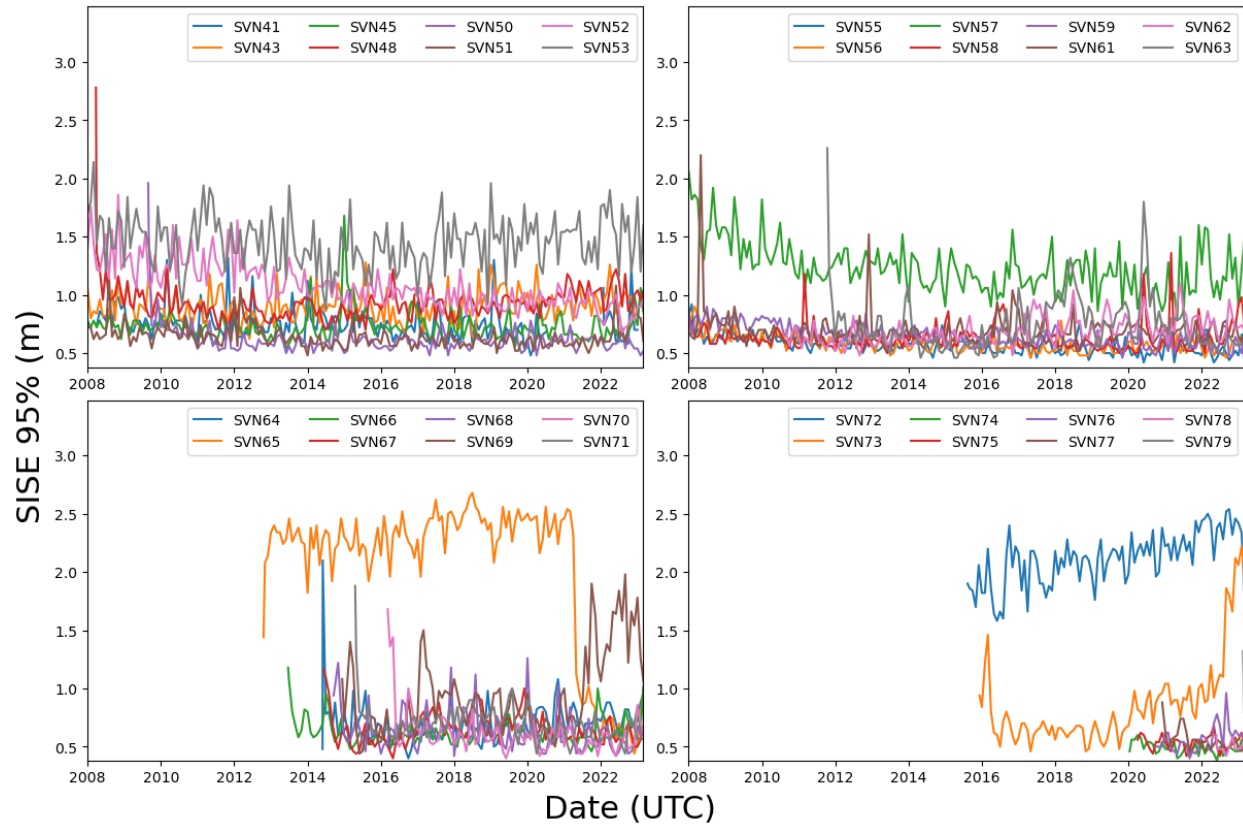
Figure 5-10. GPS Monthly 95% SISE:
January 1, 2008 to March 31, 2023

Table 5-7. GPS Monthly Mean and 95% SISE: January 1, 2008 to March 31, 2023

SVN	Max Mean (m)	Min Mean (m)	Max 95% (m)	Min 95% (m)
41	0.287	0.000	1.320	0.480
43	0.242	0.000	1.280	0.620
45	0.182	0.000	1.680	0.540
48	0.821	0.000	2.780	0.700
50	0.153	0.000	1.960	0.480
51	0.218	0.000	1.160	0.480
52	0.301	0.000	1.860	0.680
53	0.410	0.001	2.140	0.880
55	0.195	0.000	0.920	0.420
56	0.265	0.000	0.900	0.460
57	0.320	0.000	2.060	0.800
58	0.301	0.000	1.360	0.500
59	0.244	0.000	0.900	0.460
61	0.629	0.002	2.200	0.520
62	0.381	0.000	1.100	0.480
63	0.904	0.001	2.260	0.460
64	0.379	0.001	2.100	0.400
65	0.459	0.004	2.680	0.440
66	0.217	0.001	1.180	0.460
67	0.383	0.000	1.160	0.400
68	0.261	0.000	1.260	0.420
69	0.646	0.001	1.980	0.440
70	0.203	0.001	1.680	0.400
71	0.488	0.002	1.880	0.440
72	0.351	0.002	2.540	1.580
73	0.508	0.002	2.220	0.460
74	0.191	0.003	0.600	0.380
75	0.171	0.003	0.680	0.420
76	0.339	0.004	0.960	0.400
77	0.259	0.000	0.880	0.460
78	0.073	0.019	0.600	0.420
79	0.336	0.154	1.320	0.800

**Figure 5-11. Galileo Monthly Mean SISE:
January 1, 2020 to March 31, 2023**

Figure 5-12. Galileo Monthly 95% SISE:
January 1, 2020 to March 31, 2023

Table 5-8. Galileo Monthly Mean and 95% SISE: January 1, 2020 to March 31, 2023

GSAT	Max Mean (m)	Min Mean (m)	Max 95% (m)	Min 95% (m)
101	0.301	0.148	0.640	0.380
102	0.218	0.058	0.500	0.300
103	0.295	0.058	0.600	0.280
203	0.198	0.089	0.380	0.280
205	0.241	0.138	0.420	0.300
206	0.304	0.171	0.480	0.340
207	0.282	0.133	0.460	0.320
208	0.231	0.155	0.420	0.320
209	0.218	0.144	0.380	0.320
210	0.239	0.115	0.520	0.300
211	0.236	0.152	0.420	0.320
212	0.203	0.137	0.420	0.300
213	0.206	0.120	0.420	0.320
214	0.214	0.079	0.400	0.260
215	0.987	0.814	1.200	1.020
216	0.855	0.780	1.120	1.000
217	0.873	0.811	1.100	0.980
218	0.856	0.800	1.140	0.980
219	0.887	0.805	1.120	0.980
220	0.903	0.777	1.140	1.020
221	0.859	0.780	1.100	0.980
222	0.862	0.773	1.120	0.980
223	0.854	0.822	1.060	1.020

Monthly mean and 95% SISEs for each GPS satellite for this quarter are shown in Figure 5-13 and Figure 5-14. The minimum and maximum values are shown in Table 5-9. Monthly mean and 95% SISEs for each Galileo satellite for this quarter are shown in Figure 5-15 and Figure 5-16. The minimum and maximum values are shown in Table 5-10.

All the GPS means were under 0.5 m, with the high value of 0.477 m on SVN73. All the 95% values were below 2.5 m with the high value of 2.420 m on SVN72. All the Galileo means were under 1.0 m, with the high values of 0.959 m on GSAT0215. All the 95% values were below 1.2 m with the high value of 1.140 m on GSAT0215.
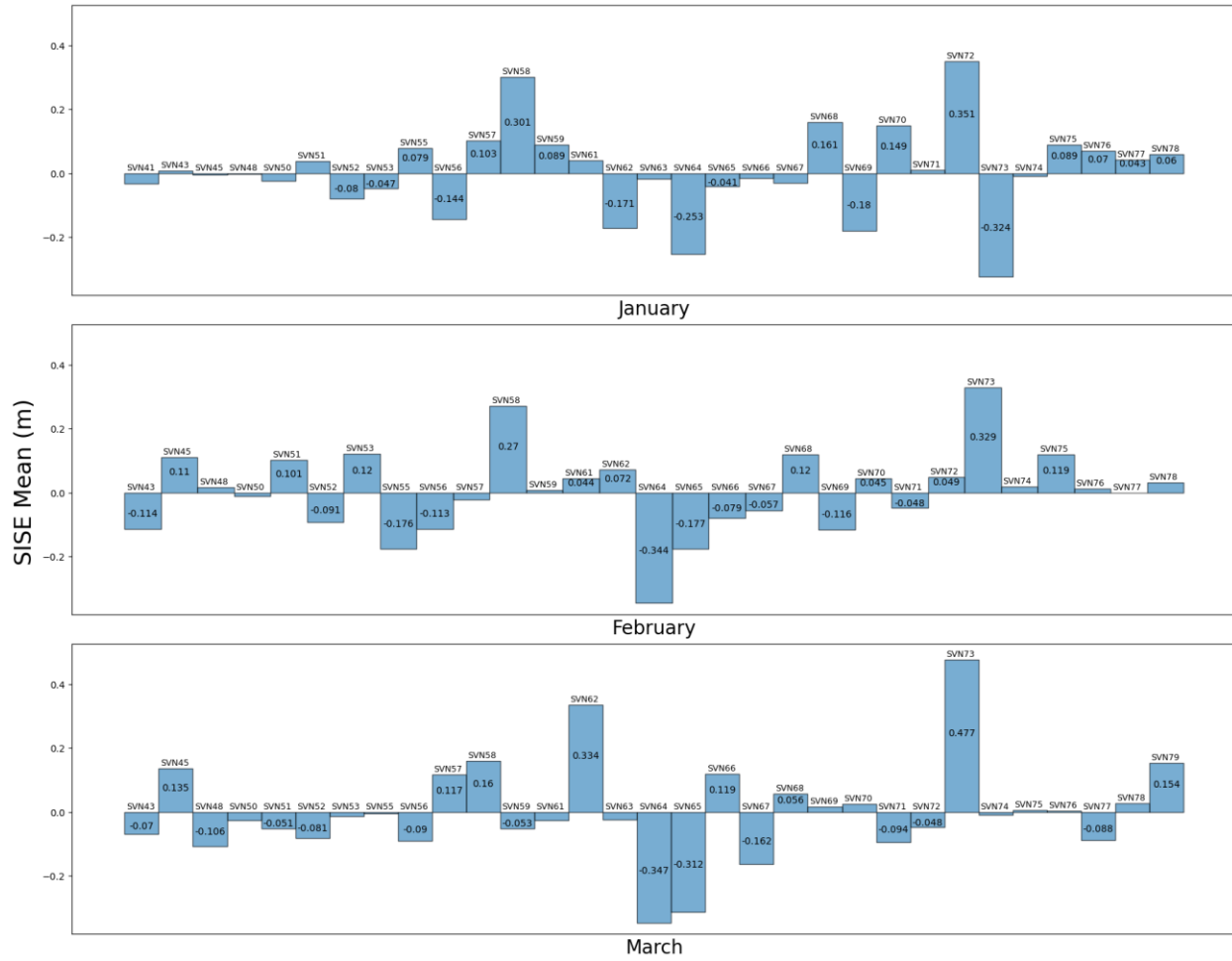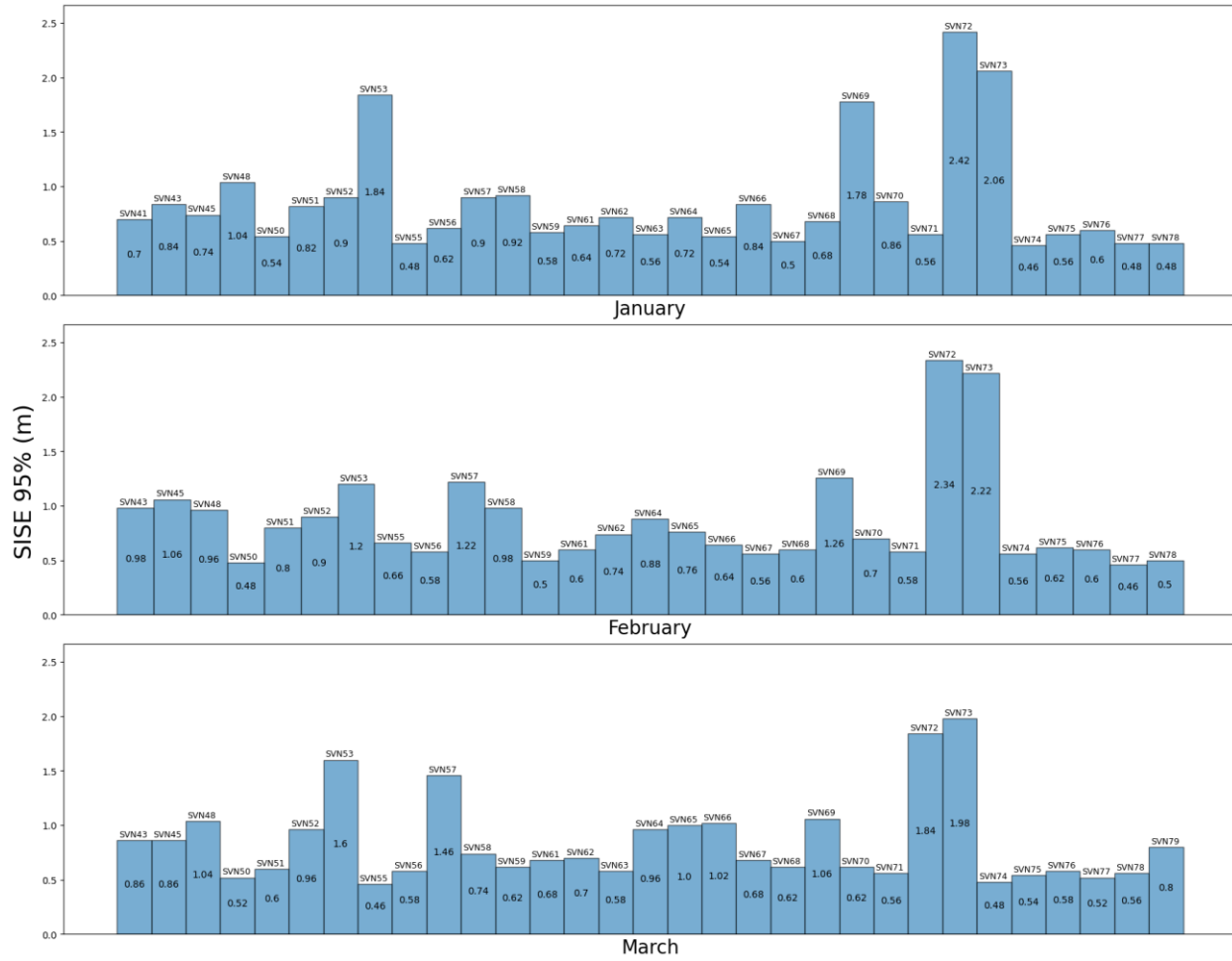
Figure 5-13. GPS Monthly Mean SISE: 1st Quarter 2023

Figure 5-14. GPS Monthly 95% SISE: 1st Quarter 2023

Table 5-9. GPS Monthly Mean and 95% SISE: 1st Quarter 2023

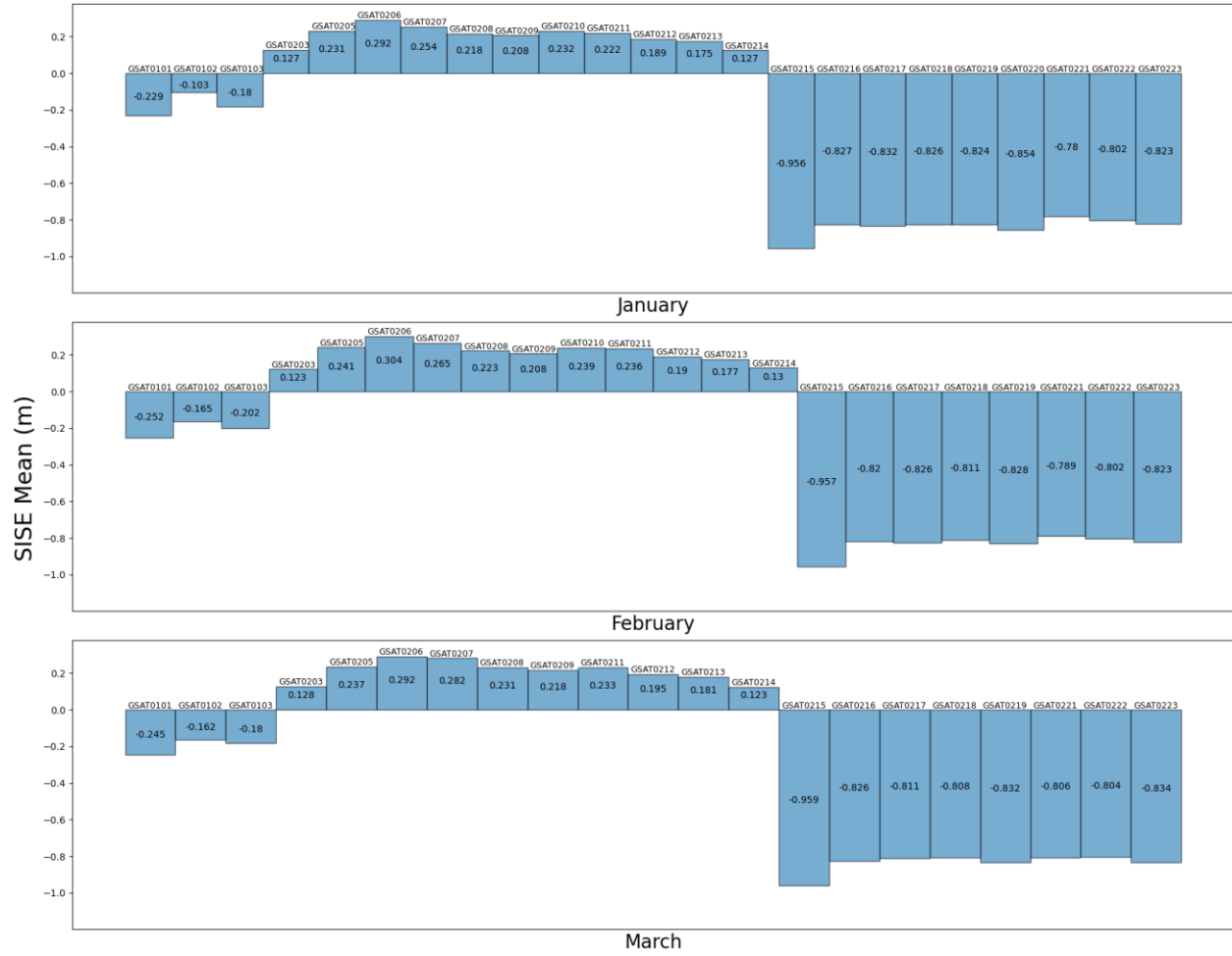| SVN	Max Mean (m)	Min Mean (m)	Max 95% (m)	Min 95% (m)
41	0.033	0.033	0.700	0.700
43	0.114	0.009	0.980	0.840
45	0.135	0.005	1.060	0.740
48	0.106	0.003	1.040	0.960
50	0.026	0.012	0.540	0.480
51	0.101	0.038	0.820	0.600
52	0.091	0.080	0.960	0.900
53	0.120	0.013	1.840	1.200
55	0.176	0.004	0.660	0.460
56	0.144	0.090	0.620	0.580
57	0.117	0.021	1.460	0.900
58	0.301	0.160	0.980	0.740
59	0.089	0.007	0.620	0.500
61	0.044	0.027	0.680	0.600
62	0.334	0.072	0.740	0.700
63	0.045	0.017	0.580	0.560
64	0.347	0.253	0.960	0.720
65	0.312	0.041	1.000	0.540
66	0.119	0.016	1.020	0.640
67	0.162	0.031	0.680	0.500
68	0.161	0.056	0.680	0.600
69	0.180	0.016	1.780	1.060
70	0.149	0.026	0.860	0.620
71	0.094	0.010	0.580	0.560
72	0.351	0.048	2.420	1.840
73	0.477	0.324	2.220	1.980
74	0.018	0.009	0.560	0.460
75	0.119	0.006	0.620	0.540
76	0.070	0.005	0.600	0.580
77	0.088	0.000	0.520	0.460
78	0.060	0.026	0.560	0.480
79	0.336	0.154	1.320	0.800

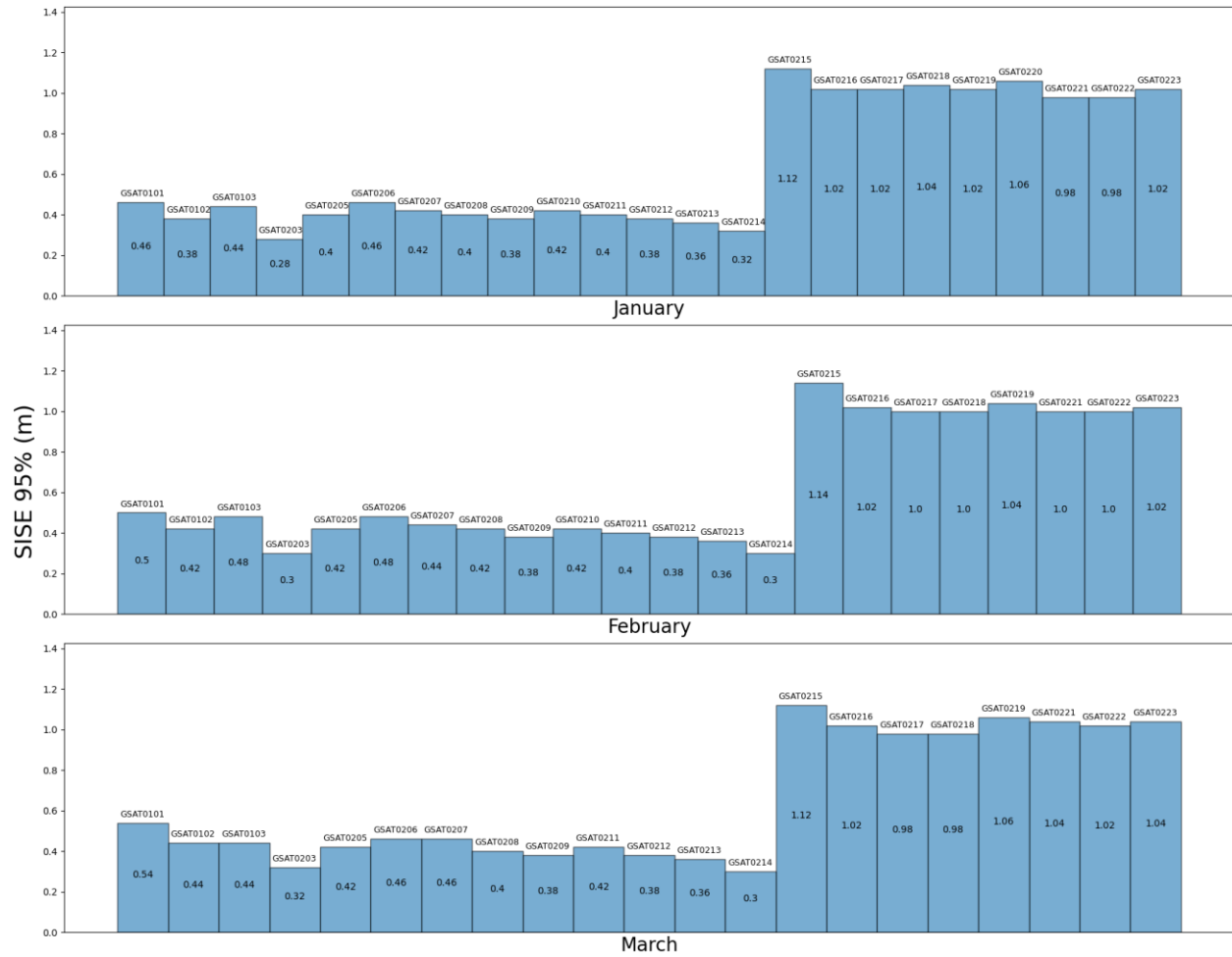**Figure 5-15. Galileo Monthly Mean SISE: 1st Quarter 2023**

Figure 5-16. Galileo Monthly 95% SISE: 1st Quarter 2023

Table 5-10. Galileo Monthly Mean and 95% SISE: 1st Quarter 2023

GSAT	Max Mean (m)	Min Mean (m)	Max 95% (m)	Min 95% (m)
101	0.252	0.229	0.540	0.460
102	0.165	0.103	0.440	0.380
103	0.202	0.180	0.480	0.440
203	0.128	0.123	0.320	0.280
205	0.241	0.231	0.420	0.400
206	0.304	0.292	0.480	0.460
207	0.282	0.254	0.460	0.420
208	0.231	0.218	0.420	0.400
209	0.218	0.208	0.380	0.380
210	0.239	0.223	0.480	0.420
211	0.236	0.222	0.420	0.400
212	0.195	0.189	0.380	0.380
213	0.181	0.175	0.360	0.360
214	0.130	0.123	0.320	0.300
215	0.959	0.956	1.140	1.120
216	0.827	0.820	1.020	1.020
217	0.832	0.811	1.020	0.980
218	0.826	0.808	1.040	0.980
219	0.832	0.824	1.060	1.020
220	0.855	0.846	1.080	1.060
221	0.806	0.780	1.040	0.980
222	0.804	0.802	1.020	0.980
223	0.834	0.823	1.040	1.020

5.3   URA Bounding of Nominal Accuracy

Nominal range error distribution is examined to evaluate how well the URA described the observed error distribution and to ensure that the Gaussian assumption is valid. MPE and UPE error distributions are evaluated in this section.

The MPE can take on the value of zero of the three orbital errors and the clock error are simultaneously zero. The MPE can switch rapidly between positive and negative values as the corresponding projections change. Therefore, the MPE distribution is bimodal with a notch at zero, and it is not expected to be Gaussian even if all underlying distributions were Gaussian. However, the UPE distribution will be Gaussian (both at individual user locations and aggregated across all user locations) if the underlying errors are Gaussian. Although the MPE distribution is not expected to be Gaussian, it is well suited to describe the tail behavior. The PDF and CDF are used to assess the error distributions of the MPE and UPE. [11].

Figure 5-17 shows the PDF MPE normalized by the broadcast URA across the GPS constellation. Figure 5-18 shows the PDF MPE normalized by σ_{URA} equal to 7.5 m across the Galileo constellation. The notch at zero is expected, as described above.

Figure 5-19 shows 1-CDF of the normalized MPE errors by GPS satellite, and Figure 5-20 shows the errors by block type. Figure 5-21 shows 1-CDF of the normalized MPE errors by Galileo satellite, and Figure 5-22 shows the errors by block type. The thick red line shows the expected value corresponding to the normal distribution with zero-mean and unit variance. This line is only extended down to the 10^{-5} probability level for GPS and 3×10^{-5} probability level for Galileo, which is the specified satellite fault rate in the GPS SPS PS and Galileo OS SDD, respectively. Gaussian bounding below this line is not required.
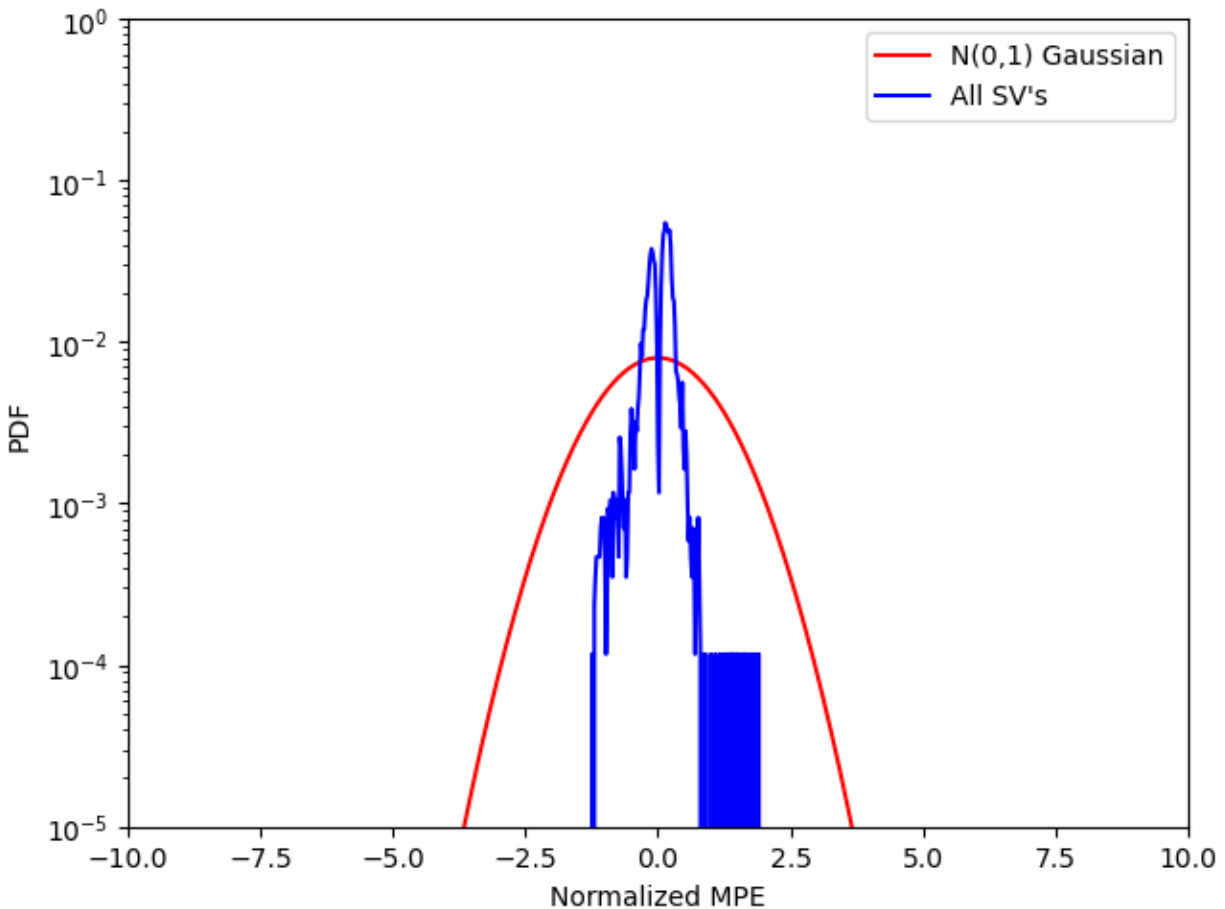

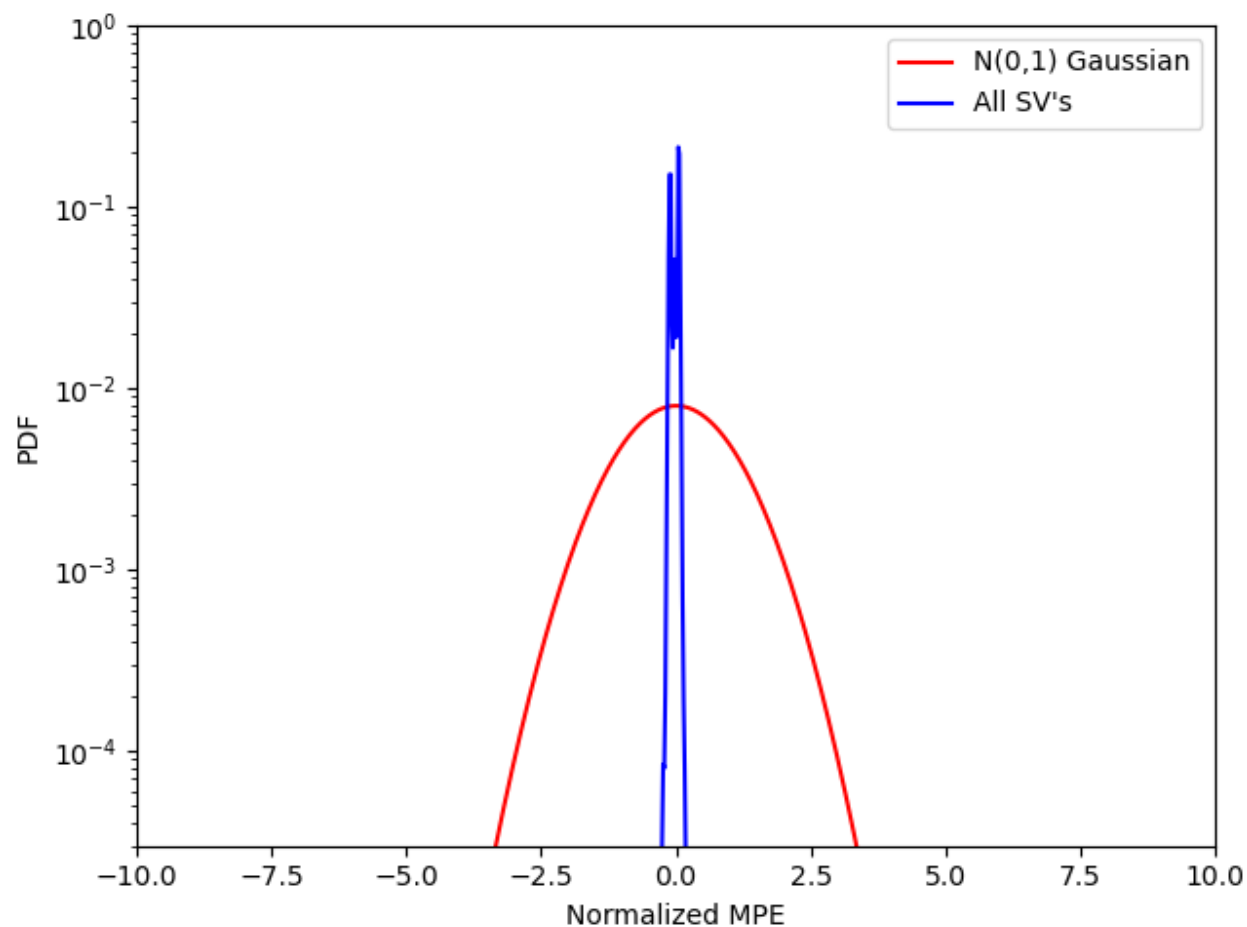**Figure 5-17. GPS PDF Normalized MPE Composite: 1st Quarter 2023**

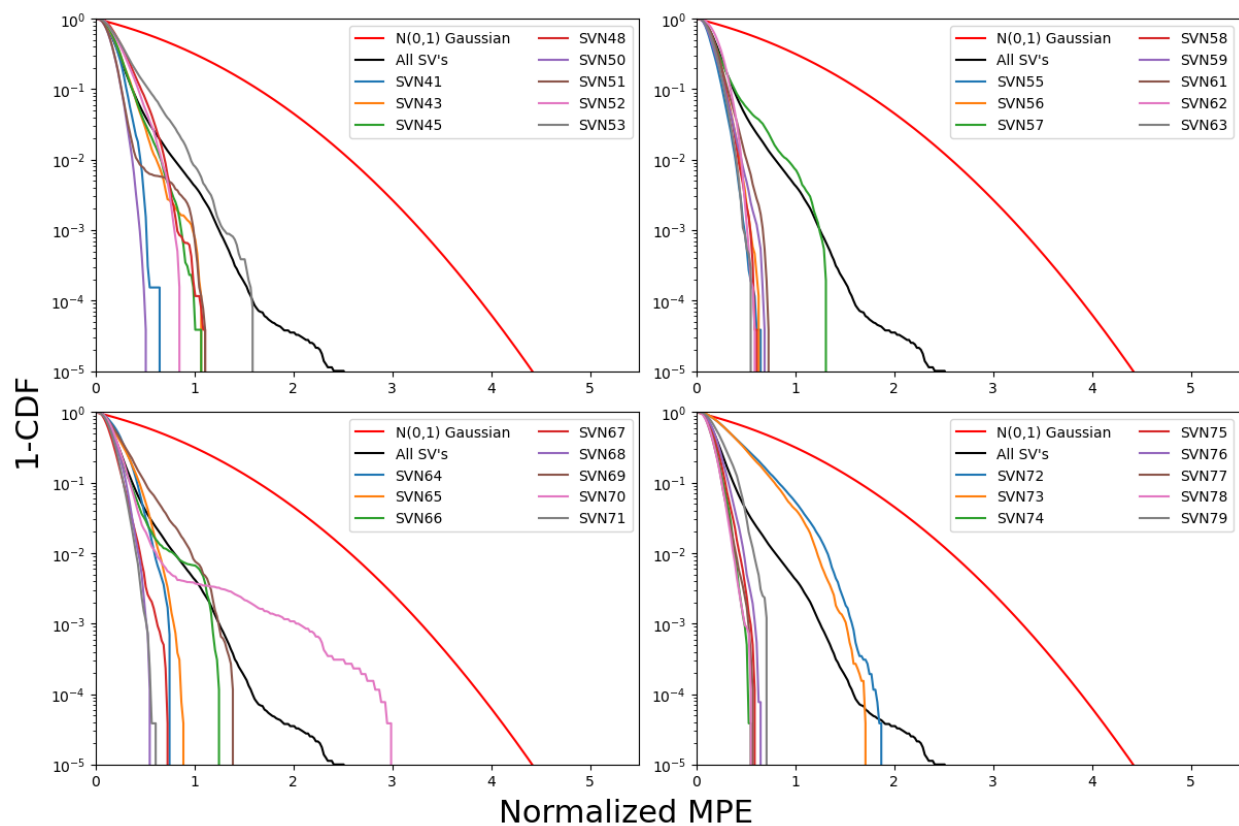**Figure 5-18. Galileo PDF Normalized MPE Composite: 1st Quarter 2023**

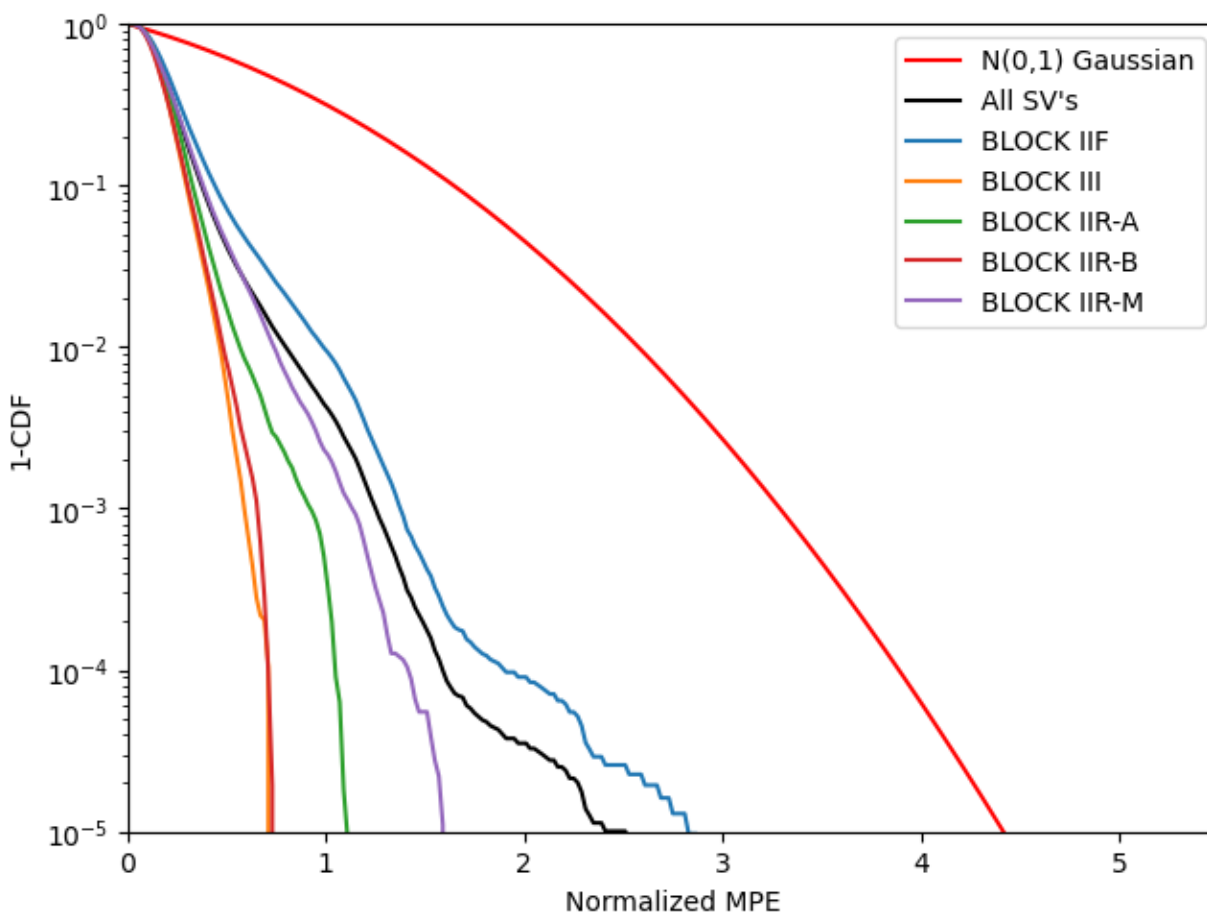**Figure 5-19. GPS 1-CDF Normalized MPE: 1st Quarter 2023**

Figure 5-20. GPS 1-CDF Normalized MPE by Block Type: 1st Quarter 2023
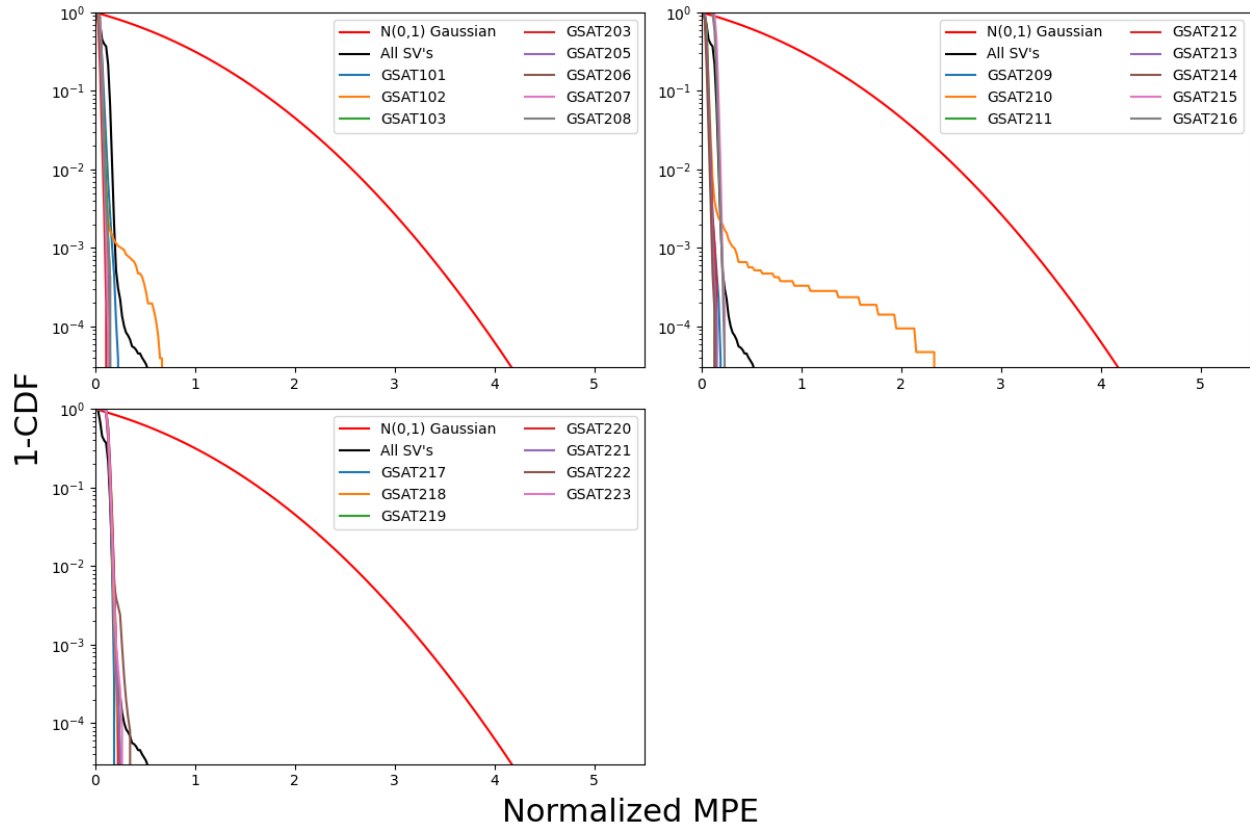
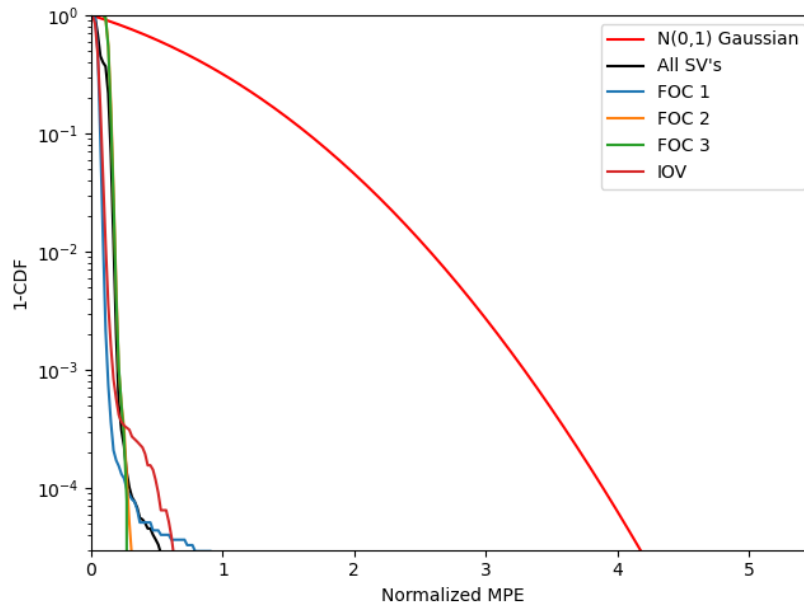**Figure 5-21. Galileo 1-CDF Normalized MPE: 1st Quarter 2023**

Figure 5-22. Galileo 1-CDF Normalized MPE by Block Type: 1st Quarter 2023

Figure 5-23 shows the PDF of the composite normalized UPEs for GPS, and Figure 5-26 shows the PDF of the composite normalized UPEs for GPS. The composite normalized UPE combines the instantaneous UPEs of all satellites at all 200 locations in each constellation. Figure 5-24 shows the 1-CDF of the normalized UPE errors combined across all 200 locations by GPS satellite, and Figure 5-25 shows them by block type. Figure 5-27 shows the 1-CDF of the normalized UPE errors combined across all 200 locations by Galileo satellite, and Figure 5-28 shows them by block type. The thick red line represents the normal distribution with zero-mean and unity variance. This line is only extended down to the 10^{-5} probability level for GPS, and 3×10^{-5} probability level for Galileo, which is the specified satellite fault rate in the GPS SPS PS and Galileo OS SDD, respectively. Gaussian bounding below this line is not required.

In this quarter, the nominal UPE errors were described conservatively by the broadcast URA for GPS satellites. The nominal errors were described conservatively by σ_{URA} of 7.5 m for Galileo satellites.
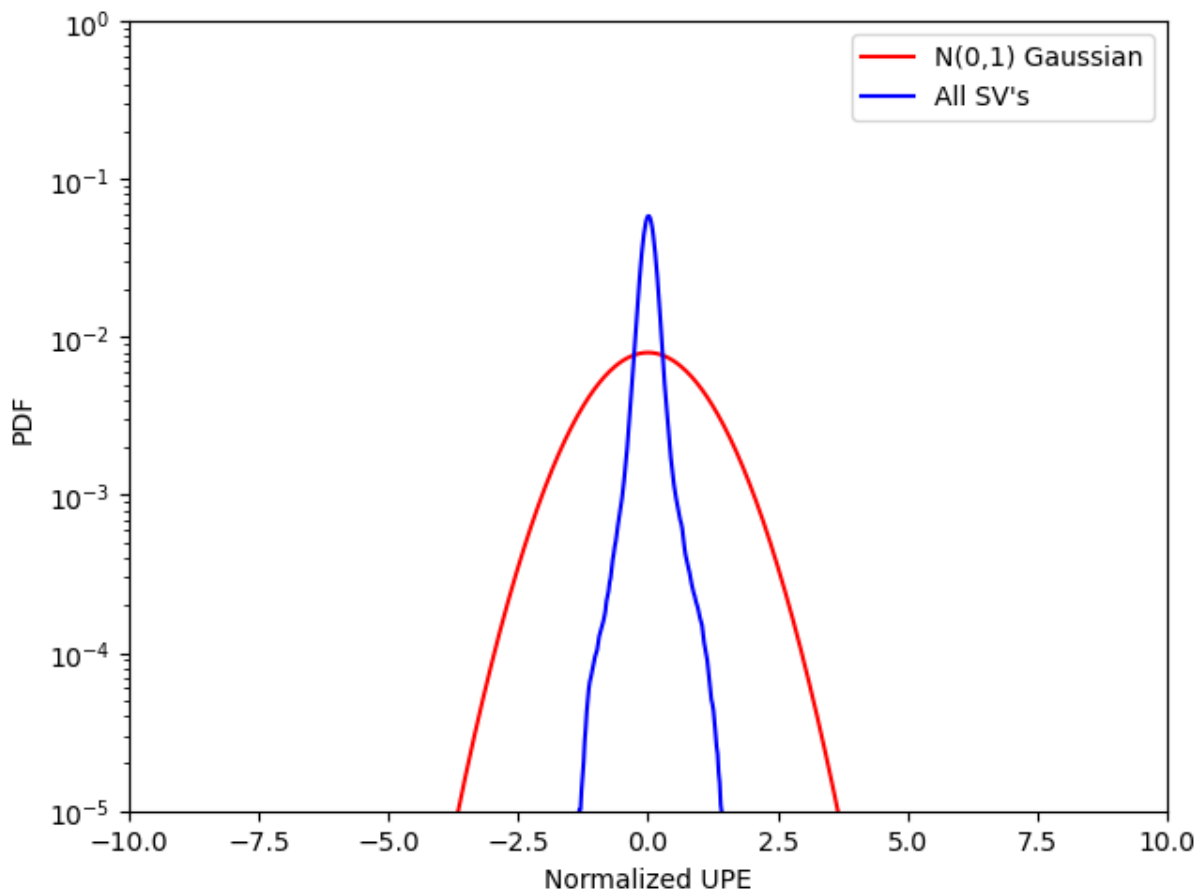

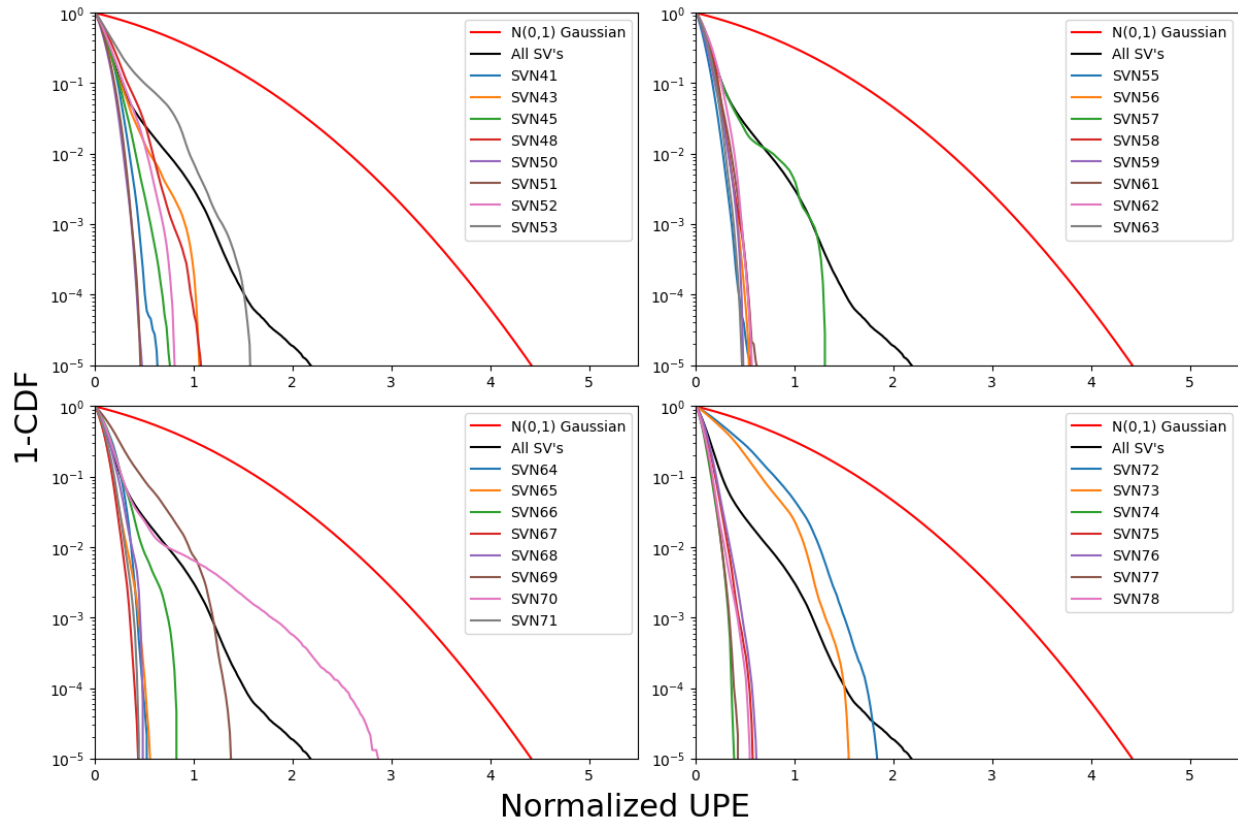**Figure 5-23. GPS PDF Normalized UPE Composite: 1st Quarter 2023**

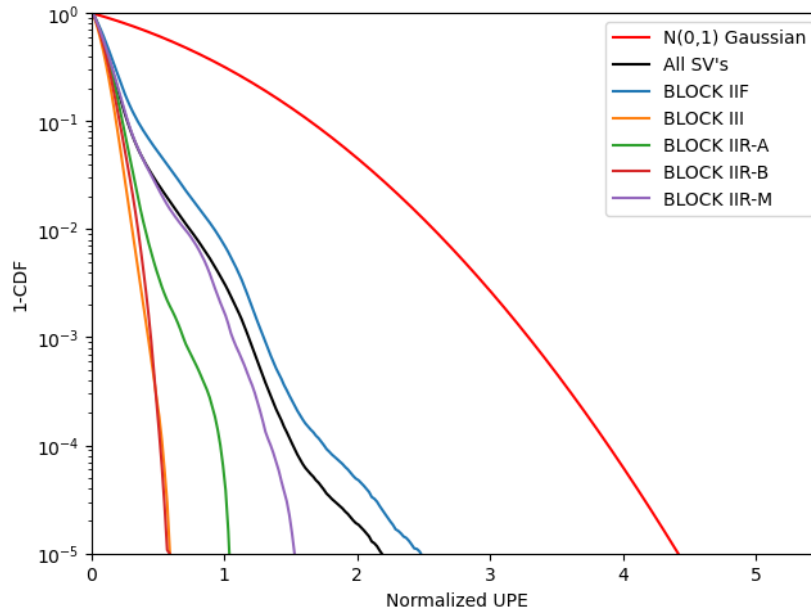**Figure 5-24. GPS 1-CDF Normalized UPE: 1st Quarter 2023**

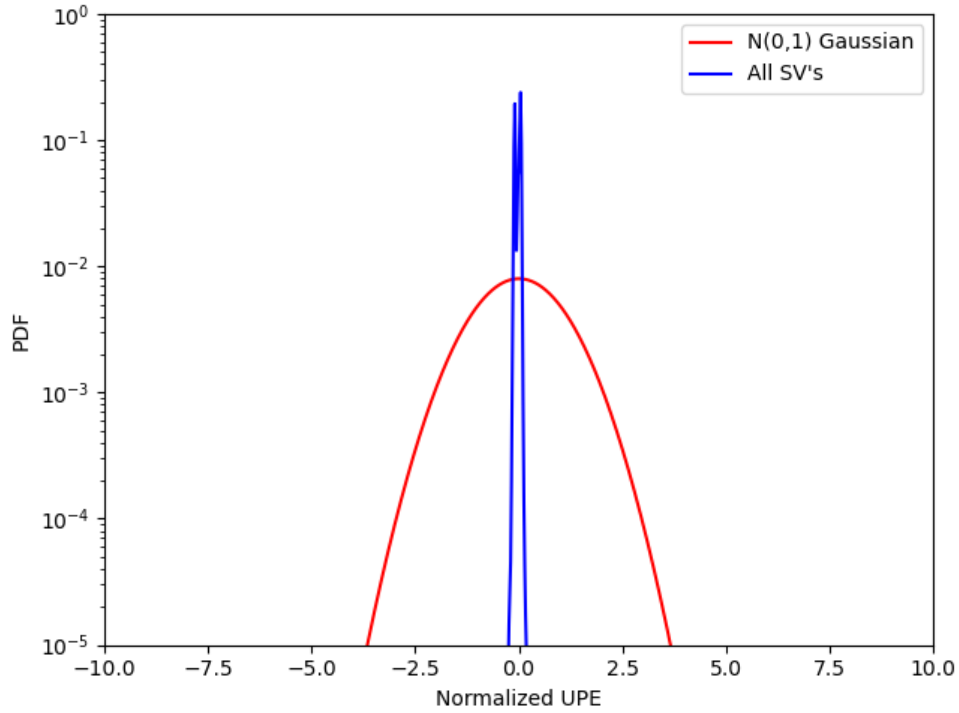**Figure 5-25. GPS 1-CDF Normalized UPE by Block Type: 1st Quarter 2023**

Figure 5-26. Galileo PDF Normalized UPE Composite: 1st Quarter 2023
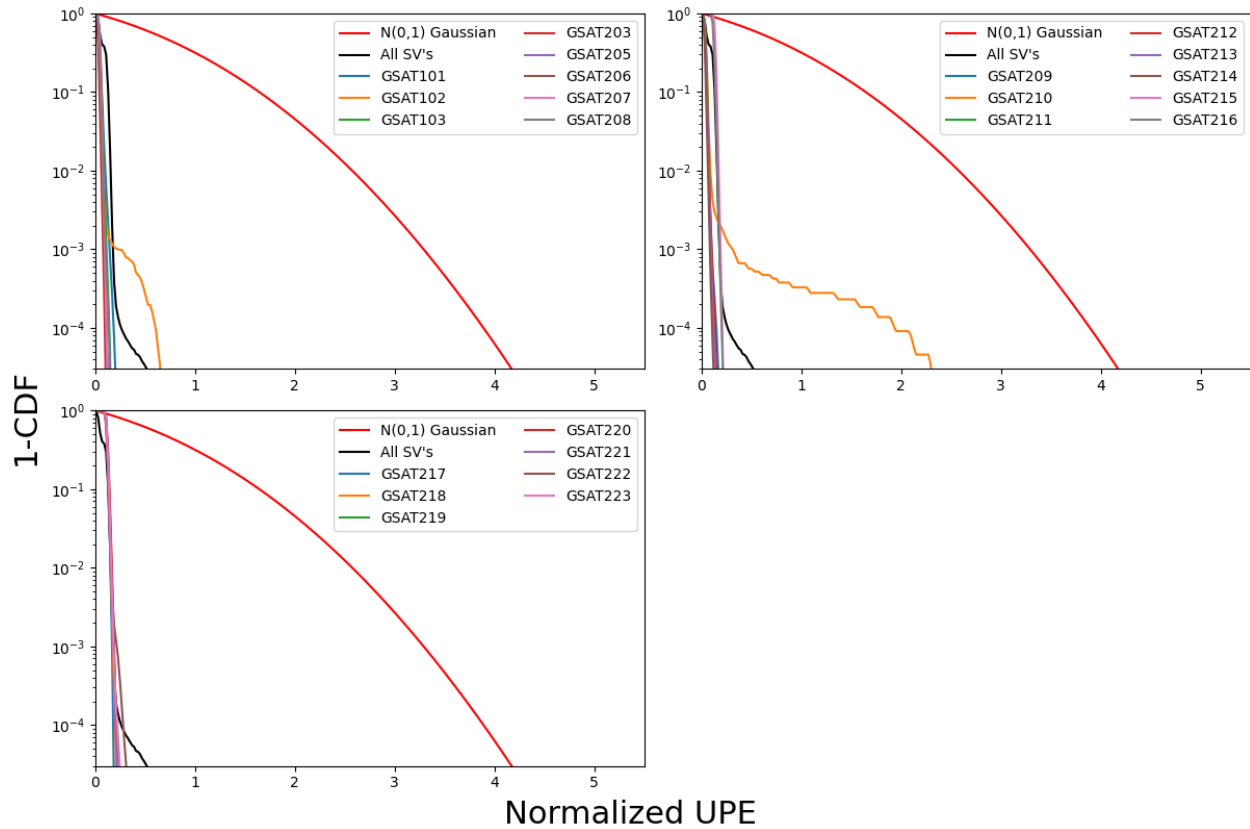

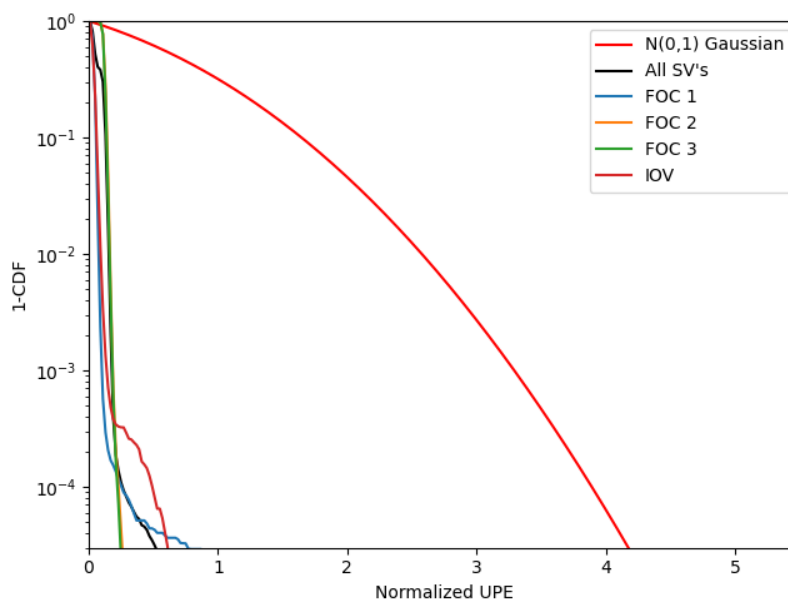**Figure 5-27. Galileo 1-CDF Normalized UPE: 1st Quarter 2023**

Figure 5-28. GPS 1-CDF Normalized UPE by Block Type: 1st Quarter 2023

The overbounding sigma and the ratio of the overbound sigma to the URA are examined to evaluate how well the nominal errors are bounded by the URA and to what degree of margin. This evaluation attempts to separate the effect of quantization of the GPS broadcast URA values from the ground system's ability to estimate the internal quantized value. Previous work has found that GPS increases the URA faster than the error actually increases, therefore, lumping all URA values together in the evaluation gave better results, which may be optimistic. More details on error bounding may be found in previous works [11, 12]. Since the GPS broadcast URA value of 2.4 m is the most frequently broadcast value at 92.752% of the time this quarter, bounding is evaluated for errors when URA is 2.4 m and for the aggregated URA values. Since there is currently no broadcast URA for Galileo, the maximum single frequency user σ_{URA} of 7.5 m is used for bounding evaluation. The ratio of less than 1 indicates the broadcast URA bounds the nominal error with a margin.

The ratio of the overbounding sigma to the broadcast URA is shown in Table 5-11 for GPS. The ratio of the overbounding sigma to σ_{URA} of 7.5 m is shown in Table 5-12 for Galileo. This ratio, or alpha value, is the smallest margin of the actual distribution to the Gaussian distribution. The overbounding sigma is formed by finding the minimum Gaussian value that bounds the SISE CDF for each satellite at each error value. Alpha is the ratio between the points on the Gaussian curve and observed error curve with the smallest difference. Small regions of the curves are ignored during evaluation to account for convergence around the origin. The Y-axis data must be between 0.000095 and 0.5, and the X-axis data must be between 0.1 and 4.42 for GPS. The Y-axis data must be between 0.000095 and 0.5, and the X-axis data must be between 0.1 and 4.17 for Galileo. Figure 5-29 shows the ratio of the bounding sigma for URA at 2.4 m only. Figure 5-30 shows the ratio of the bounding sigma for σ_{URA} at 7.5 m only. Table 5-11 shows the ratio of the bounding sigma to the broadcast URA of 2.4 m and for the combined broadcast URA values for each GPS

satellite. Table 5-12 shows the ratio of the bounding sigma to σ_{URA} of 7.5 m for each Galileo satellite.

For GPS this quarter, the alpha values for the URA of 2.4 m only were very similar to the alpha values of the combined URAs. The largest alpha value for GPS was 0.568 on SVN70, and the largest alpha value for Galileo was 0.499 on GSAT0210.

Table 5-11. GPS Ratio of Bounding Sigma to URA: 1st Quarter 2023

| SVN	Ratio for URA=2.4 m Only	Ratio for All URAs
41	0.151	0.151
43	0.261	0.259
45	0.243	0.240
48	0.239	0.239
50	0.116	0.113
51	0.285	0.277
52	0.212	0.211
53	0.376	0.372
55	0.125	0.125
56	0.136	0.136
57	0.364	0.359
58	0.155	0.147
59	0.152	0.152
61	0.167	0.167
62	0.200	0.195
63	0.139	0.139
64	0.211	0.205
65	0.197	0.197
66	0.329	0.327
67	0.168	0.167
68	0.151	0.151
69	0.373	0.368
70	0.568	0.568
71	0.129	0.129
72	0.477	0.476
73	0.454	0.450
74	0.118	0.118
75	0.135	0.135
76	0.146	0.146
77	0.132	0.132
78	0.123	0.123
79	0.174	0.180
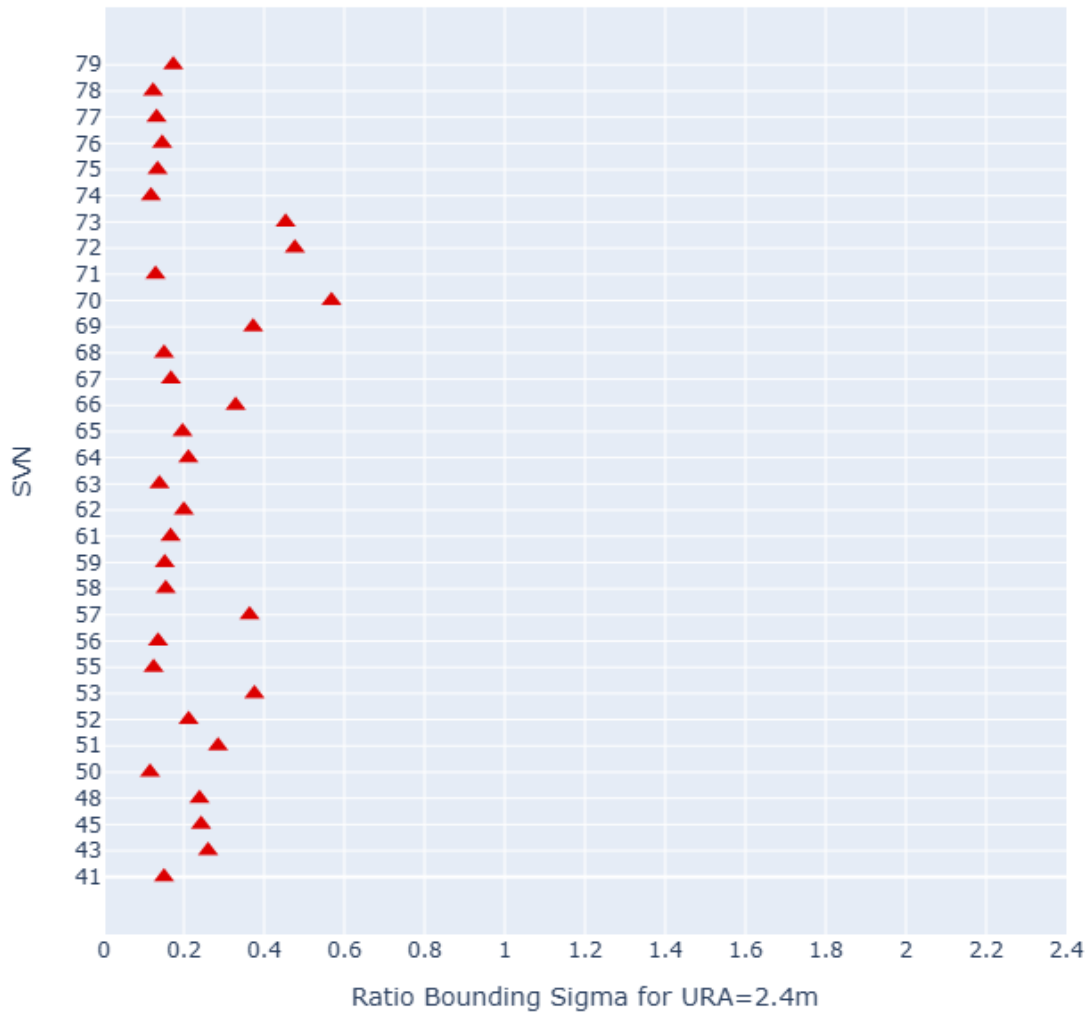
Figure 5-29. GPS Ratio of Bounding Sigma for URA=2.4 m: 1st Quarter 2023

Table 5-12. Galileo Ratio of Bounding Sigma to URA: 1st Quarter 2023

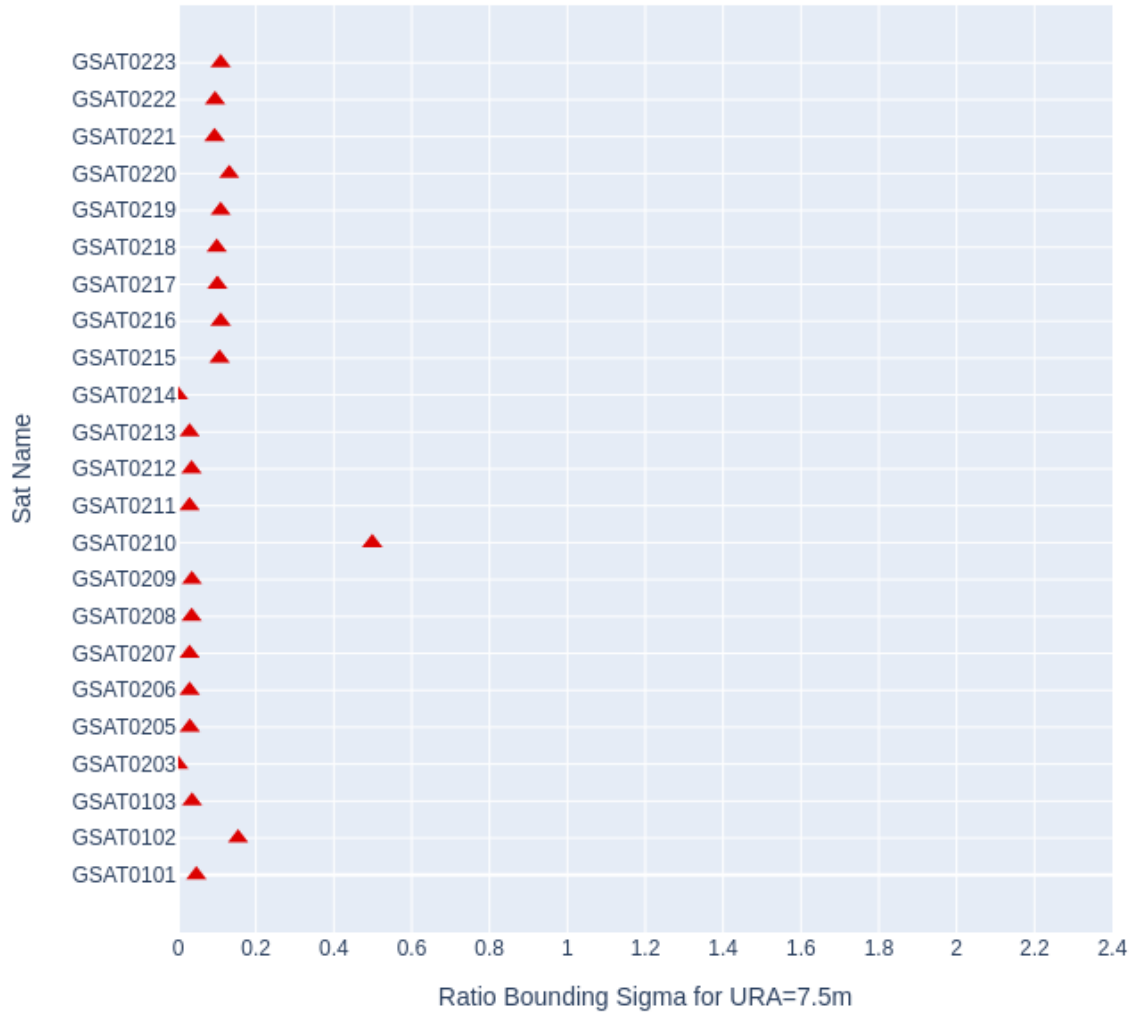| SVN	Ratio for URA=7.5 m
GSAT0101	0.047
GSAT0102	0.154
GSAT0103	0.036
GSAT0203	0.000
GSAT0205	0.030
GSAT0206	0.030
GSAT0207	0.029
GSAT0208	0.035
GSAT0209	0.035
GSAT0210	0.499
GSAT0211	0.029
GSAT0212	0.034
GSAT0213	0.029
GSAT0214	0.000
GSAT0215	0.106
GSAT0216	0.109
GSAT0217	0.101
GSAT0218	0.099
GSAT0219	0.109
GSAT0220	0.131
GSAT0221	0.094
GSAT0222	0.095
GSAT0223	0.109

Figure 5-30. Galileo Ratio of Bounding Sigma for URA=7.5 m: 1st Quarter 2023

5.4 URA Bounding of Nominal Position Accuracy

Nominal position errors are examined to ensure that individual satellite range errors, when combined, do not create position errors larger than the ones expected, assuming independent Gaussian range errors with a standard deviation given by the URA (the nominal error model), which is what the user assumes. It is important to assess the nominal position bounding for any possible user weights, because not all users will apply the same weights when combining the range errors. This can be achieved by examining the sum of the squares (SS) of the URA-normalized satellite range errors.

The SS has two important properties. First, it is chi-square distributed assuming the nominal error model. Second, its square root is an upper bound of the ratio between the user error and the standard deviation as computed assuming the nominal error model [13, 14]. The observed SS distribution is expected to be well bounded by a chi-square distribution. If it is not, it means that the correlation in the measurements will cause the position errors to be larger than expected for some users. If the observed distribution is bounded by a unit Gaussian (for a range of probabilities), then the position errors are guaranteed to be bounded by a Gaussian with the expected standard deviation.

The SS is computed at each time epoch at the 200 user locations. It is obtained by subtracting a common-mode error from each SISE (because this common error has no effect on the position error), normalizing each SISE by the URA, and summing the squares of the resulting ratios.

Figure 5-31 and Figure 5-32 show the 1-CDF of the SS sample distribution (blue line), chi-square distribution (dotted red line), and zero mean unit Gaussian distribution (solid red line) for GPS and Galileo, respectively. The SS sample distribution is bounded by the chi-square distribution with ample margin. This indicates that the errors are consistent with an error model that is bounded by the nominal error model. In addition, the SS sample distribution is bounded by the Gaussian for all probabilities below 70%. This corresponds to the point in the CDFs in Figure 5-31 and Figure 5-32 where the unit Gaussian (solid red curve) crosses the SS statistic (blue curve). Using the result outlined above, this means that those probabilities derived from the nominal error model are guaranteed to bound the distribution of the position error. This indicates that the unfaulted positioning errors are bounded by the nominal error model with significant margin.
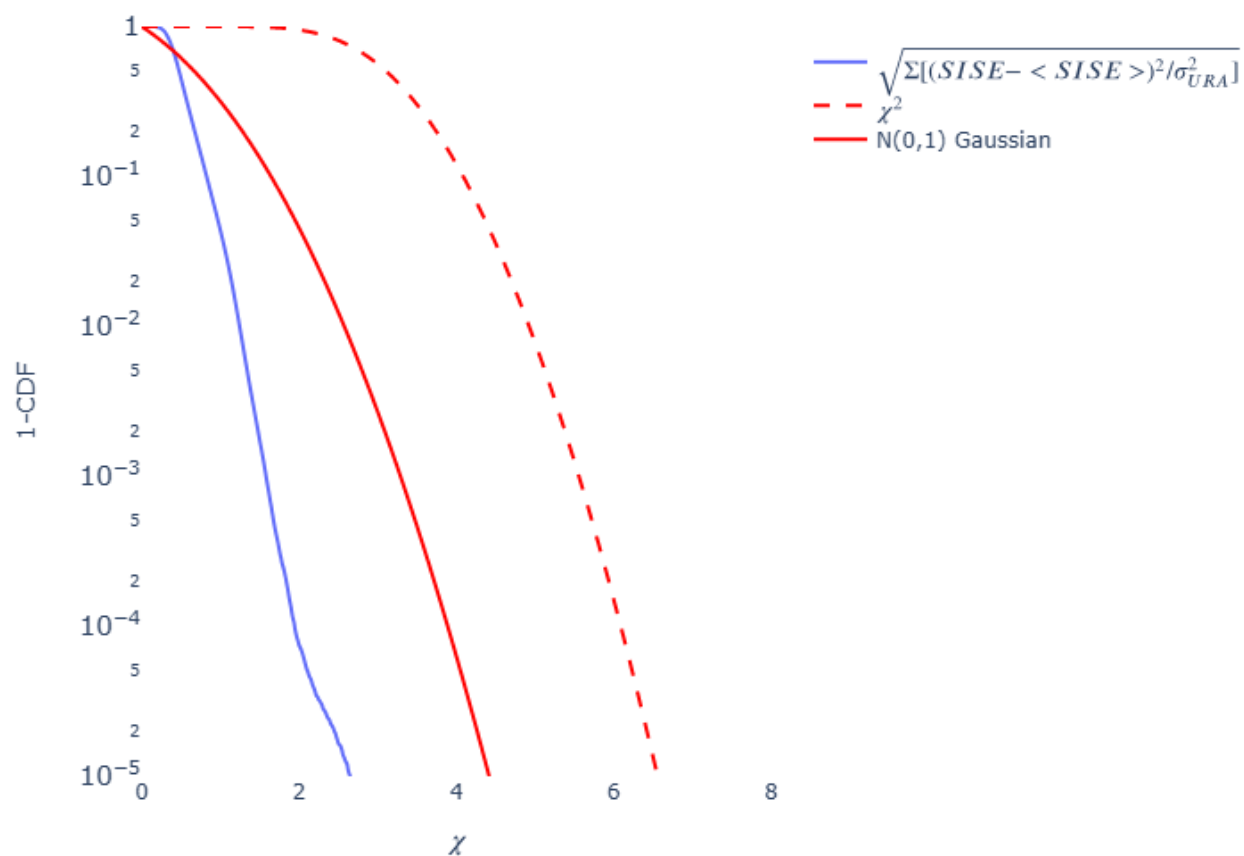
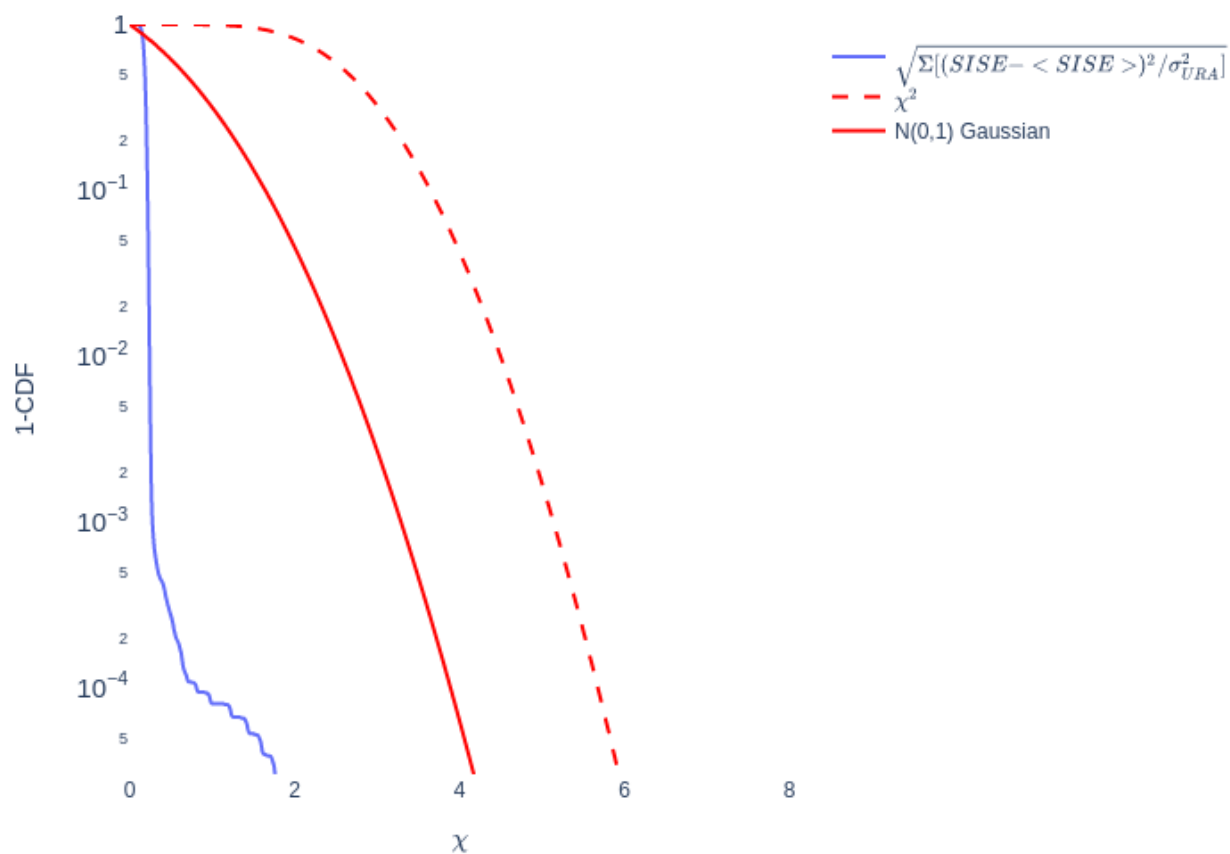**Figure 5-31. GPS 1-CDF Chi-Square of Normalized UPEs: 1st Quarter 2023**

Figure 5-32. Galileo 1-CDF Chi-Square of Normalized UPEs: 1st Quarter 2023

6.   FAULT PROBABILITY

At the time of this writing, no final decision was made on the format of the ISM message. In particular, fault rate information may be conveyed as an actual fault rate or as a probability of failure over a specified period of time. In this report, we present the fault rate only. The state fault probability can be obtained easily by multiplying the fault rate by the MFD. As the standardization process evolves, the approved approach or approaches will be presented in this section.

The critical fault parameters for ARAIM are the R_{sat} and P_{sat}, the R_{const} or P_{const}, and the MFD. These three parameters are based upon CSP commitments and are supported by observational history. This section assesses the GPS and Galileo constellation observed fault rates and MFD to ensure they are consistent with CSP commitments (see Table 2-1 and Table 2-2). The consistency requires the evaluation of GPS and Galileo fault history, including satellite and constellation fault rates based on actual historical data.

Table 6-1 lists the known GPS constellation faults and durations since January 1, 2008. The first five faults have been discussed in a previous paper [13]. Table 6-2 lists the known Galileo constellation faults and durations since January 1, 2020.

Table 6-1. GPS Faults From January 1, 2008 to March 31, 2023 [13]

SVN	PRN	Date	Time of Fault (UTC)	Fault Duration	Description
25	25	6/26/2009	09:05 – 09:45	40 minutes	A clock jumped 20 m at 09:05 causing the error to exceed 4.42*URA. URA was 2.4 m. Orbit was not affected, and the satellite was healthy. At 09:45, 155 of 156 IGS stations stopped tracking the satellite. Normal tracking of the satellite was resumed at 10:23 with a new ephemeris update that set the satellite to unhealthy. The lone receiver had only started tracking the satellite at 09:44:30 with discontinuities in pseudorange.
38	8	11/5/2009	18:45 – 19:02	17 minutes	A clock ramp occurred at 18:15 causing the error to exceed 4.42*URA at 18:44:45. URA was 2.4 m. Orbit was not affected and the satellite was healthy. All 135 IGS stations stopped tracking the satellite at 19:02. At approximately 19:28, regular transmission resumed with a new ephemeris update that set the satellite to unhealthy.

SVN	PRN	Date	Time of Fault (UTC)	Fault Duration	Description
30	30	02/22/2010	20:45 – 20:52	7 minutes	A clock ramp occurred at 20:30 causing the error to exceed 4.42*URA at 20:45. URA was 2.4 m. Orbit was not affected and the satellite was healthy. All 108 IGS stations stopped tracking the satellite at 20:52. At approximately 2:15, regular transmission resumed with a new ephemeris update that set the satellite to unhealthy.
39	9	04/25/2010	19:40 – 19:55	15 minutes	At 19:26, a new ephemeris update introduced a 40 m cross-track error with the URA=2.4 m. The MPE error barely exceeded the 4.42*URA at 19:40. The fault was corrected at 19:55 with a new ephemeris update. The satellite health was set to healthy the entire time.
59	19	06/17/2012	00:10 – 00:36	26 minutes	At 00:10, a new ephemeris update introduced a 1700 m cross-track error with the URA=2.4 m. The MPE error exceeded the 4.42*URA. The fault was corrected at 00:37 with a new ephemeris update. The satellite health was set to healthy the entire time.
58	12	10/02/2022	14:50 – 16:00	70 minutes	A clock ramp began at 07:30 causing the error to exceed 4.42*URA at 14:50. The fault was corrected at 16:00 with a new ephemeris update. The satellite health was set to healthy the entire time.
63	1	01/25/2023	16:15 – 19:15	180 minutes	At 16:00, a new ephemeris update introduced a 27m clock jump causing the MPE to exceed 4.42*URA at 16:15. The fault was corrected at 19:15 with a new ephemeris update. The satellite health was set to healthy the entire time.

Five of the seven known faults lasted less than 1 hour, and the average across all seven faults was 29.17 minutes. Therefore, the committed value of MFD of 1 hour appears to be valid and conservative.

Table 6-2. Galileo Faults From January 1, 2020 to March 31, 2023

Satellite Name	SVID	Date	Time of Fault (UTC)	Fault Duration
GSAT0102	12	01/21/2021	09:05 – 09:45	40 minutes
GSAT0210	1	09/05/2021	18:45 – 19:02	17 minutes
GSAT0210	1	04/29/2022	20:45 – 20:52	7 minutes
GSAT0210	1	08/31/2022	20:45 – 20:52	7 minutes

All four faults lasted less than 1 hour, and the average across all four faults was 29.17 minutes.

Independent, single satellite faults are referred to as narrow faults, and simultaneous or overlapping satellite faults that originate from a common cause within a single constellation, are referred to as wide faults. The narrow fault rate computation for GPS uses a 30-satellite constellation and takes into account the historical satellite faults listed in Table 6-1. The narrow fault rate computation for Galileo uses a 22-satellite constellation and takes into account the historical satellite faults listed in Table 6-2. Figure 6-1 shows the times of historical single-fault events and their effect on the fault rate for GPS, and Figure 6-2 shows the times of historical single-fault events and their effect on the fault rate for Galileo. The rates are shown for different time windows computed at 6-month increments. The fault rate determination for GPS has been discussed in previous work [15], and the method recommended in the previous work suggested taking the maximum value of the sliding 48-month average, which corresponds to a number well below 10^{-5}.

In this quarter, a fault was observed on SVN63 (PRN01) with an approximate duration of 180 minutes.
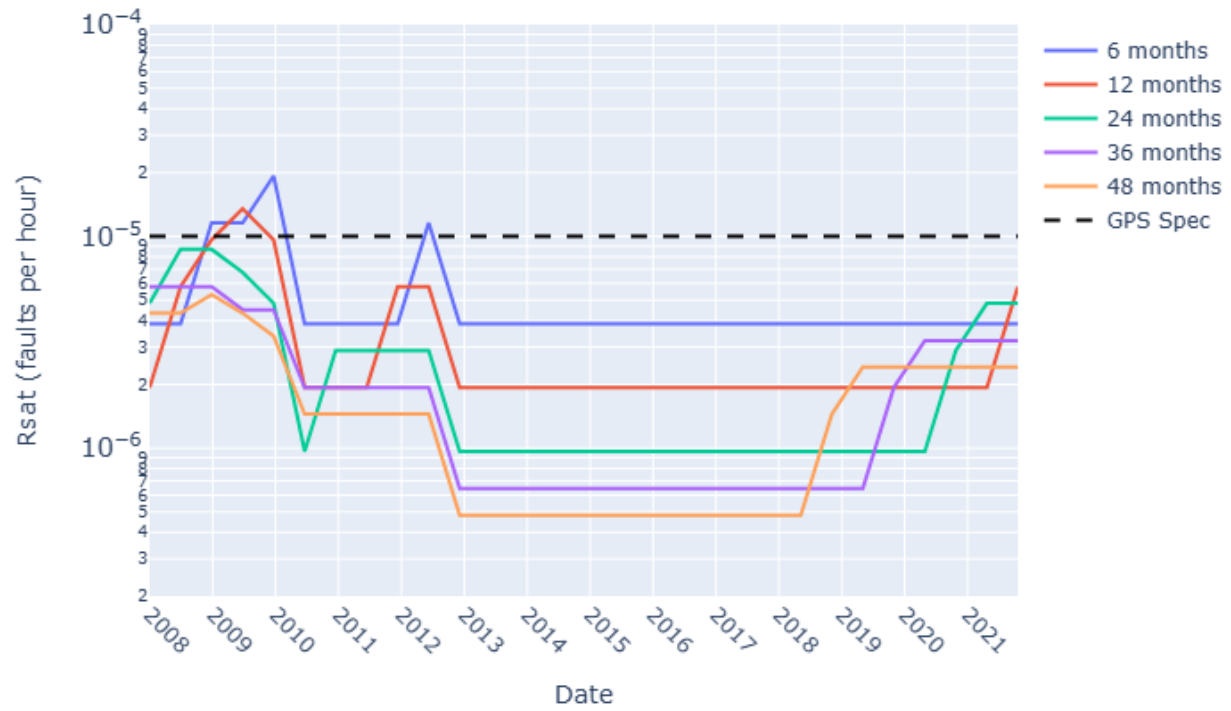
Figure 6-1. GPS Estimated Satellite Narrow Fault Rate
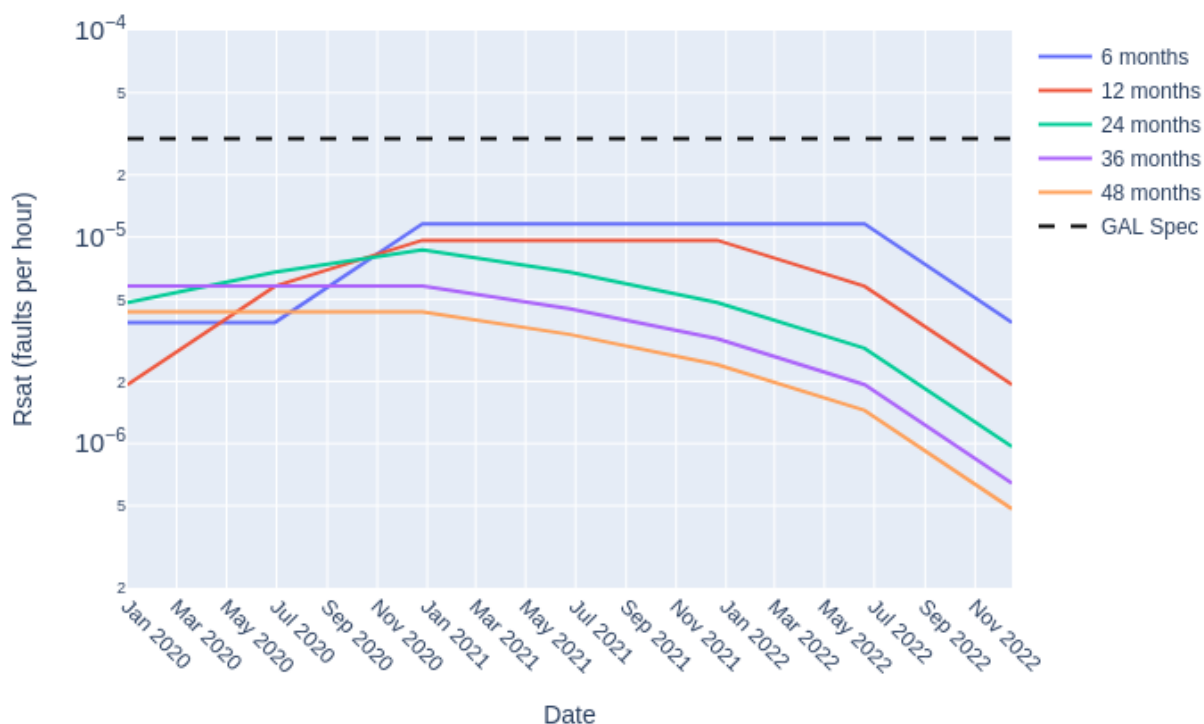
Figure 6-2. Galileo Estimated Satellite Narrow Fault Rate

7. EVENTS

Table 7-1 lists all GPS events for this quarter, and Table 7-2 lists all the Galileo events for the quarter. Events include potential SIS anomalies and any other issues that occurred during this reporting period. Analyses of events that merit more detailed investigations are documented in the individual ARAIM PAN reports, which can be found at https://www.nstb.tc.faa.gov/araim-archive.html and by hyperlink in Table 7-1 and Table 7-2.

Table 7-1. GPS Events

SVN	PRN	Start	End	Description
41	22	11-Jan-23 03:44 UTC	11-Jan-23 09:28 UTC	SVN41 (PRN22) was set unusable. See NANU2023002.
41	22	23-Jan-23 20:16 UTC	N/A	SVN41 (PRN22) was set decommissioned. See NANU2023006.
63	1	25-Jan-23 16:15 UTC	25-Jan-23 19:15 UTC	SVN63 (PRN01) Normalized Max Projected Error exceeded 4.42 while the navigation health status was set to healthy.
63	1	25-Jan-23 16:00 UTC	26-Jan-23 15:41 UTC	SVN63 (PRN01) was set unusable. See NANU2023008.
79	28	N/A	N/A	SVN79 (PRN28) was set launched. See NANU2023007.
62	25	26-Jan-23 15:35 UTC	26-Jan-23 21:23 UTC	SVN62 (PRN25) was set unusable. See NANU2023009.
63	1	28-Jan-23 15:00 UTC	02-Feb-23 22:22 UTC	SVN63 (PRN01) was set unusable. See NANU2023011.
79	28	16-Feb-23 20:56 UTC	N/A	SVN79 (PRN28) was set usable. See NANU2023013.
56	16	16-Feb-23 21:52 UTC	17-Feb-23 03:29 UTC	SVM56 (PRN16) was set unusable. See NANU2023014.
52	31	28-Feb-23 00:15 UTC	28-Feb-23 10:19 UTC	SVN52 (PRN31) was set unusable. See NANU2023016.
48	7	09-Mar-23 21:49 UTC	10-Mar-23 03:42 UTC	SVN48 (PRN07) was set unusable. See NANU2023018.

Table 7-2. Galileo Events

Name	SVID	Start	End	Description
GSAT 0219	36	17-Jan-23 01:55 UTC	21-Jan-23 20:52 UTC	GALILEO SATELLITE GSAT0219 (ALL SIGNALS) IS USABLE SINCE/AS OF 2023-01-21 BEGINNING 20:52 UTC. PAYLOAD ON PHM CLOCK. GALILEO SATELLITE GSAT0219 (ALL SIGNALS) WAS UNAVAILABLE FROM 2023-01-17 BEGINNING 01:55 UTC.
GSAT 0203	26	24-Jan-23 05:30 UTC	28-Jan-23 15:22 UTC	GALILEO SATELLITE GSAT0203 (ALL SIGNALS) IS USABLE SINCE/AS OF 2023-01-28 BEGINNING 15:22 UTC. PAYLOAD ON PHM CLOCK. GALILEO SATELLITE GSAT0203 (ALL SIGNALS) WAS UNAVAILABLE FROM 2023-01-24 BEGINNING 05:30 UTC.
GSAT 0220	13	31-Jan-23 04:30 UTC	05-Feb-23 15:22 UTC	GALILEO SATELLITE GSAT0220 (ALL SIGNALS) IS USABLE SINCE/AS OF 2023-02-05 BEGINNING 15:22 UTC. PAYLOAD ON PHM CLOCK. GALILEO SATELLITE GSAT0220 (ALL SIGNALS) WAS UNAVAILABLE FROM 2023-01-31 BEGINNING 04:30 UTC.
GSAT 0221	15	07-Feb-23 04:01 UTC	11-Feb-23 14:42 UTC	GALILEO SATELLITE GSAT0221 (ALL SIGNALS) IS USABLE SINCE/AS OF 2023-02-11 BEGINNING 14:42 UTC. PAYLOAD ON PHM CLOCK. GALILEO SATELLITE GSAT0221 (ALL SIGNALS) WAS UNAVAILABLE FROM 2023-02-07 BEGINNING 04:01 UTC.
GSAT 0210	1	28-Feb-23 08:21 UTC	09-Mar-23 11:10 UTC	GALILEO SATELLITE GSAT0210 (ALL SIGNALS) IS USABLE SINCE/AS OF 2023-03-09 BEGINNING 11:10 UTC. PAYLOAD ON RAFS CLOCK. GALILEO SATELLITE GSAT0210 (ALL SIGNALS) WAS UNAVAILABLE FROM 2023-02-28 BEGINNING 08:21 UTC.
GSAT 0220	13	20-Feb-23 18:54 UTC	11-Mar-23 06:36 UTC	GALILEO SATELLITE GSAT0220 (ALL SIGNALS) IS USABLE SINCE/AS OF 2023-03-11 BEGINNING 06:36 UTC. PAYLOAD ON PHM CLOCK. GALILEO SATELLITE GSAT0220 (ALL SIGNALS) WAS UNAVAILABLE FROM 2023-02-20 BEGINNING 18:54 UTC.
GSAT 0206	30	14-Mar-23 03:30 UTC	18-Mar-23 15:22 UTC	GALILEO SATELLITE GSAT0206 (ALL SIGNALS) IS USABLE SINCE/AS OF 2023-03-18 BEGINNING 15:22 UTC. PAYLOAD ON PHM CLOCK. GALILEO SATELLITE GSAT0206 (ALL SIGNALS) WAS UNAVAILABLE FROM 2023-03-14 BEGINNING 03:30 UTC.
GSAT 0210	1	20-Mar-23 13:18 UTC	20-Mar-23 16:15 UTC	SHORT TERM OUTAGE ON GALILEO SATELLITE GSAT0210 (ALL SIGNALS) HAS BEEN RECOVERED. PAYLOAD ON RAFS CLOCK. GALILEO SATELLITE GSAT0210 (ALL SIGNALS) WAS UNAVAILABLE FROM 2023-03-20 BEGINNING 13:18 UTC UNTIL 2023-03-20 ENDING 16:15 UTC.
GSAT 0217	27	21-Mar-23 03:30 UTC	25-Mar-23 19:24 UTC	GALILEO SATELLITE GSAT0217 (ALL SIGNALS) IS USABLE SINCE/AS OF 2023-03-25 BEGINNING 19:24 UTC. PAYLOAD ON PHM CLOCK. GALILEO SATELLITE GSAT0217 (ALL SIGNALS) WAS UNAVAILABLE FROM 2023-03-21 BEGINNING 03:30 UTC.
N/A	N/A	27-Mar-23 07:30 UTC	28-Mar-23 07:00 UTC	THE TEST CAMPAIGN IS COMPLETED AS OF 2023-03-28 07:00 UTC. THE SIGNAL IN SPACE REMAINED COMPLIANT WITH THE PUBLISHED OS AND HAS SERVICE DEFINITION DOCUMENTS AND SIGNAL IN SPACE INTERFACE CONTROL DOCUMENTS DURING THE WHOLE TEST.
GSAT 0210	1	23-Mar-23 17:37 UTC	29-Mar-23 16:18 UTC	GALILEO SATELLITE GSAT0210 (ALL SIGNALS) IS USABLE SINCE/AS OF 2023-03-29 BEGINNING 16:18 UTC. PAYLOAD ON RAFS CLOCK. GALILEO SATELLITE GSAT0210 (ALL SIGNALS) WAS UNAVAILABLE FROM 2023-03-23 BEGINNING 17:37 UTC.
GSAT 0205	24	28-Mar-23 04:45 UTC	01-Apr-23 15:26 UTC	GALILEO SATELLITE GSAT0205 (ALL SIGNALS) IS USABLE SINCE/AS OF 2023-04-01 BEGINNING 15:26 UTC. PAYLOAD ON PHM CLOCK. GALILEO SATELLITE GSAT0205 (ALL SIGNALS) WAS UNAVAILABLE FROM 2023-03-28 BEGINNING 04:45 UTC.

8.   REFERENCES

1. EU Agency for the Space Programme (EUSPA), "Galileo Open Service Signal-In-Space Document (OS SIS ICD)," Issue 2.1, November 2023, available at https://www.gsc-europa.eu/sites/default/files/sites/all/files/Galileo_OS_SIS_ICD_v2.1.pdf

2. ARAIM Concept of Operation, Working Group C Service Evolution Subgroup, April 23, 2018.

3. Department of Defense, "Global Positioning System Standard Position Service Performance Standard," 5th Edition, April 2020.

4. EU Agency for the Space Programme (EUSPA), "Galileo Open Service Service Definition Document (OS SDD)," Issue 1.3, November 2023, available at https://www.gsc-europa.eu/sites/default/files/sites/all/files/Galileo-OS-SDD_v1.3.pdf

5. International GNSS Service (IGS), "RINEX The Receiver Independent Exchange Format," Version 3.05, December 1, 2020, https://files.igs.org/pub/data/format/rinex305.pdf

6. National Geospatial-Intelligence Agency, NGA/GPS 5 Minute Ephemeris SP3 Format Description, https://earth-info.nga.mil/index.php?dir=gnss&action=gnss

7. National Aeronautics and Space Administration, CDDIS, https://cddis.nasa.gov/

8. Scripps Orbit and Permanent Array Center/California Spatial Reference Center, http://sopac-csrc.ucsd.edu/

9. National Geospatial-Intelligence Agency, GPS and Earth Orientation Products, https://earth-info.nga.mil/GandG/update/index.php?action=home#tab_gnss

10. Heng, L., "Safe Satellite Navigation with Multiple Constellations: Global Monitoring of GPS and GLONASS Signal-in-Space Anomalies," 2012.

11. Walter, T., Gunning, K., Phelts, E., and Blanch, J., "Validation of Unfaulted Error Bounds for ARAIM," NAVIGATION Journal of The Institute of Navigation, February 2018.

12. Blanch, J., Walter, T., and Enge, P., "Gaussian Bounds of Sample Distributions for Integrity Analysis," in IEEE Transactions on Aerospace and Electronic Systems, Vol. 55, No. 4, pp. 1806-1815, Aug. 2019, doi: 10.1109/TAES.2018.2876583.

13. Walter, T. and Blanch, J., "Characterization of GNSS Clock and Ephemeris Errors to Support ARAIM," Proceedings of the ION 2015 Pacific PNT Meeting, Honolulu, Hawaii, April 2015

14. Walter, T., Blanch, J., Enge, P., "Evaluation of Signal in Space Error Bounds to Support Aviation Integrity," NAVIGATION, Journal of The Institute of Navigation, Vol. 57, No. 2, Summer 2010, pp. 101-113.

15. Walter, T., Blanch, J., Joerger, M., and Pervan, B., "Determination of Fault Probabilities for ARAIM," Proceedings of IEEE/ION PLANS 2016, Savannah, Georgia, April 2016.

APPENDIX A: GLOSSARY AND ACRONYMS

ARAIM	Advanced Receiver Autonomous Integrity Monitoring
b_{nom0}	URA-independent overbound of nominal range bias error
CDDIS	Crustal Dynamics Data Information System (IGS archive site)
CDF	Cumulative Distribution Function
cm	Centimeter
CODE	Center for Orbit Determination in Europe
CSP	Constellation Service Provider
ECEF	Earth-Centered, Earth-Fixed
FAA	Federal Aviation Administration
FOC	Full Operational Capability
GNSS	Global Navigation Satellite Systems
GPS	Global Positioning System
GSAT	Galileo Satellite
IAURA	Integrity Assured User Range Accuracy. The IAURA is a conservative representation of the upper bound on each satellite's expected RMS URE performance over the curve fit interval represented by the NAV data from which the URA is read.
ICD	Interface Control Document
IGS	International GNSS Service
IODE	Issue Of Data Ephemeris
ISM	Integrity Support Message
m	Meter
MFD	Mean Fault Duration
MPE	Maximum Projected Error
MSI	Misleading Signal-in-Space Information

NANU   Notice Advisory to Navstar Users

NAPA   No Accuracy Prediction Available

NGA   National Geospatial-Intelligence Agency

NTE   Not to Exceed (i.e., tolerance limit)

OS   Open Service

PAN   Performance Analysis Report

P_{const} Probability of multiple satellites being in a common-cause MSI faulted state at a given time.

PDF   Probability Density Function

PRN   Pseudo-Random Noise

PS   Performance Standard

P_{sat} Probability of a satellite being in an MSI faulted state at a given time

RAC   Radial-along track-cross track (Orbital coordinate system)

RINEX   Receiver Independent Exchange

R_{sat} Rate of a single satellite fault

SDD   Service Definition Document

SF   Single-Frequency

SIS   Signal-in-Space

SISA   Signal-in-Space Accuracy

SISE   Signal-in-Space Range Error

SOPAC   Scripps Orbit and Permanent Array Center (IGS archive site)

SP3   Standard Product #3

SPS   Standard Positioning Service. The GPS broadcast signals, as defined in IS-GPS-200 and IS-GPS-705, providing constellation performance to peaceful civil, commercial, and scientific users, as established in the SPS Performance Standard (SPS PS), in accordance with U.S. Government policy.

SS   Sum of the Squares

SV	Space Vehicle
SVN	Space Vehicle Number
t_{CORREL}	Correlation Time Constant
TSTTOM	Time Since Transmission Time of Message
UMSI	Unalerted Misleading Signal Information.
UPE	User Projected Error
URA	User Range Accuracy. The URA is a conservative representation of each satellite's expected RMS URE performance over the curve fit interval represented by the NAV data from which the URA is read.
URE	User Range Error
U.S.	United States
UTC	Coordinated Universal Time
WAAS	Wide Area Augmentation System
γ_{nom}	URA-dependent overbound of nominal range bias errors

APPENDIX B: SVN63 (PRN01) Fault

Figure B-1 is made up of four subplots, which show the SVN63 (PRN01) Daily Summary January 25, 2023. The first subplot shows the MPE and UPE normalized by the URA. Yellow indicates the normalized UPE across the 200 locations. The two red lines are the maximum and minimum normalized UPE, and the blue line is the normalized MPE.

The second subplot shows the IODE and satellite health. Green indicates when the satellite was healthy, and red indicates when it was unhealthy.

The third subplot shows the time since transmission time of message (TSTTOM) and precise data health. The blue line is the fit interval (in seconds). The green line shows the TSTTOM of the most recent ephemeris data when the precise product was available, and the red line shows when the precise product was flagged unhealthy. The black glyph marks the ephemeris update at 2-hour intervals, and the purple glyph shows the ephemeris update outside the 2-hour interval.

The fourth subplot shows the orbit and clock errors. The black line shows the broadcast URA values in meters. The blue line shows the radial error, the orange line shows the along-track error, the green line shows the cross-track error, and the red line shows the clock error.

On January 25th, 2023, the normalized MPE on PRN01 exceeded 4.42 for approximately 3 hours from 16:15 to 19:15 UTC. The satellite maintained a healthy status during the event as shown in the second subplot. The satellite also remained within the 4 hour (14,400 seconds) fit interval as shown in the third subplot. The fault began approximately 15 minutes after the initial broadcast of IODE 54 and remained in a faulted state for the duration of the subsequent broadcast of IODE 62. The fault event concluded when the status of the satellite changed to unhealthy with the start of IODE 12. The source of the high error can be attributed to the large clock jump shown by the red trace in the fourth subplot at 16:15 UTC. The precise position provider flagged the satellite at this time, indicating a clock event, and is shown as a red mark in the third subplot.
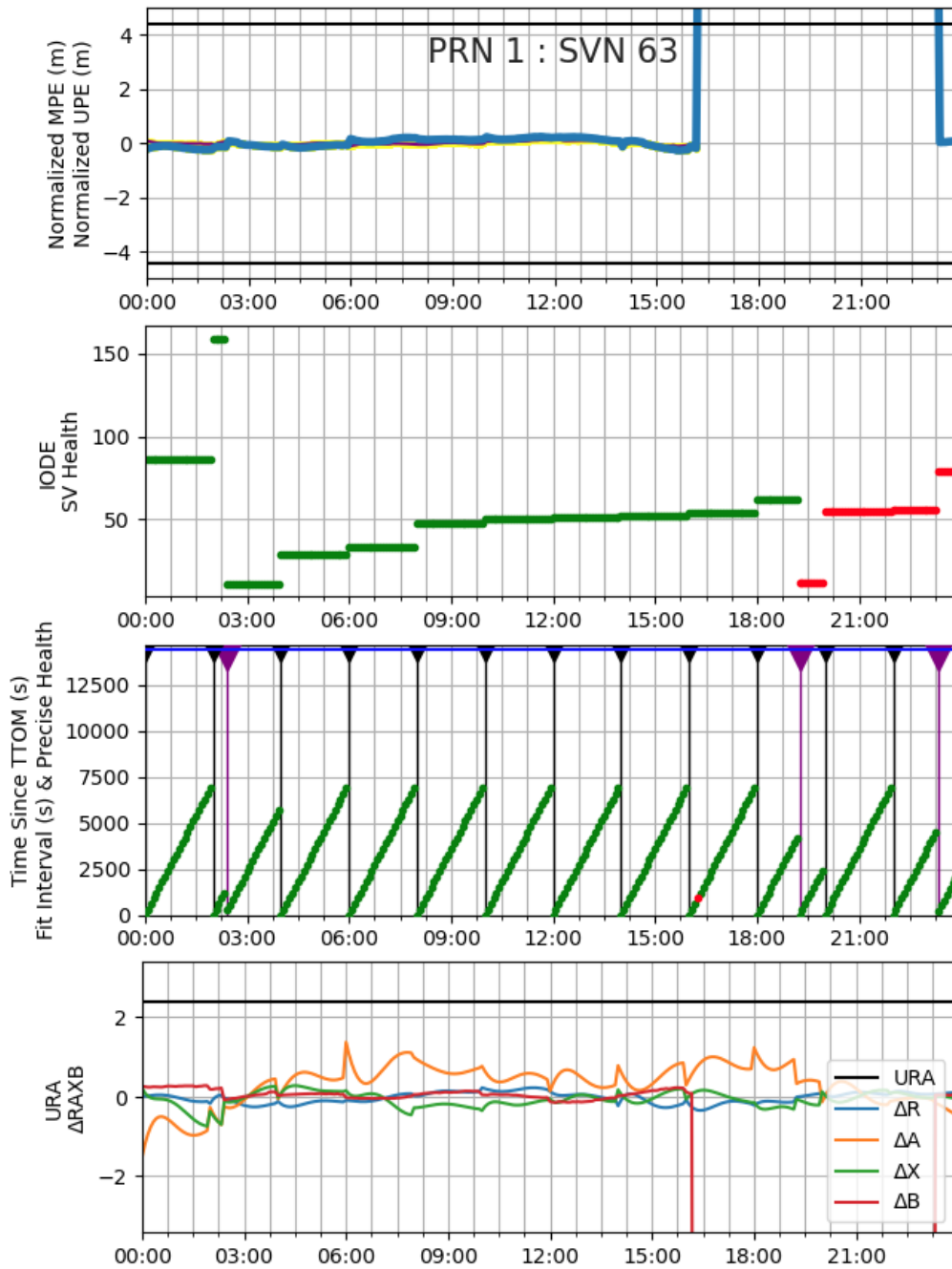
Figure B-1. SVN63 (PRN01) Daily Summary January 25, 2023